Genetic modification of flavone biosynthesis in rice enhances biofilm formation of soil diazotrophic bacteria and biological nitrogen fixation

Dawei Yan[1], Hiromi Tajima[1], Lauren C. Cline[2], Reedmond Y. Fong[3], Javier I. Ottaviani[3,4], Howard-Yana Shapiro[1] and Eduardo Blumwald[1],*

[1]Department of Plant Sciences, University of California, Davis, California, USA
[2]Bayer Crop Science, St. Louis, Missouri, USA
[3]Department of Nutrition, University of California, Davis, California, USA
[4]Mars Inc., McLean, Virginia, USA

Summary

Improving biological nitrogen fixation (BNF) in cereal crops is a long-sought objective; however, no successful modification of cereal crops showing increased BNF has been reported. Here, we described a novel approach in which rice plants were modified to increase the production of compounds that stimulated biofilm formation in soil diazotrophic bacteria, promoted bacterial colonization of plant tissues and improved BNF with increased grain yield at limiting soil nitrogen contents. We first used a chemical screening to identify plant-produced compounds that induced biofilm formation in nitrogen-fixing bacteria and demonstrated that apigenin and other flavones induced BNF. We then used CRISPR-based gene editing targeting apigenin breakdown in rice, increasing plant apigenin contents and apigenin root exudation. When grown at limiting soil nitrogen conditions, modified rice plants displayed increased grain yield. Biofilm production also modified the root microbiome structure, favouring the enrichment of diazotrophic bacteria recruitment. Our results support the manipulation of the flavone biosynthetic pathway as a feasible strategy for the induction of biological nitrogen fixation in cereals and a reduction in the use of inorganic nitrogen fertilizers.

Introduction

Nitrogen is an essential element for plant growth. Plants cannot directly assimilate the abundant nitrogen gas available in our atmosphere; instead, they rely on the uptake of inorganic forms of nitrogen, such as ammonium and nitrate, from the soil. Modern agriculture is heavily dependent on the application of chemical fertilizers to improve maximum productivity. Approximately, half of the N fertilizer (Fowler et al., 2013) used in agriculture is lost to the fields where it is applied through volatilization into the atmosphere, increasing the N_2O concentrations in the atmosphere, contributing to greenhouse gas emissions and global warming (Thompson et al., 2019). N fertilizers also leach from the soil profile to underground water systems, contributing to the eutrophication of water bodies (Withers et al., 2014). Nitrate contamination of public water resources increased significantly with the use of N fertilizers and may pose serious health challenges to the general population (Essien et al., 2020). In addition, the production of industrial ammonia from atmospheric nitrogen (Haber-Bosch process) is energy-intensive and the production of nitrogen fertilizers is predicted to consume 2% of global energy by 2050 (Glendining et al., 2009).

There is a growing need to develop sustainable alternative agricultural practices that reduce the extensive use of inorganic nitrogen fertilizers. These alternative approaches include making possible the conversion of atmospheric N_2 to ammonia by bacteria (Biological Nitrogen Fixation, BNF) reducing the need for nitrogen fertilizers in agriculture. N_2-fixing bacteria (diazotrophs) produce nitrogenase, the enzyme complex that mediates the reduction of N_2 to ammonia. Diazotrophs can interact with plant roots symbiotically or not symbiotically. In symbiotic interactions, such as those between legumes and rhizobia, bacteria are located in differentiated root cells, called nodules, where nitrogen fixation occurs (Udvardi and Poole, 2013). Two main experimental strategies aimed at engineering nitrogen fixation in cereal plants have been reported: (i) expression of bacterial nitrogenase genes in plants and (ii) developing a legume-like root nodule symbiosis in cereal crop plants. Nevertheless, stable expression of the nitrogenase or the generation of nodules in cereals has not been achieved yet.

The interactions between plant roots and the microbe-rich soil environment are critical for plant fitness. It is estimated that plants extrude up to 20% of their fixed carbon (Haichar et al., 2016) and many of these compounds (organic acids, amino acids, phenolics, secondary metabolites, etc.) help shape the microbes in the rhizosphere and rhizoplane (Haichar et al., 2016). The root–bacteria interactions in the soil are also supported by the formation of biofilms, a bacteria self-produced matrix of extracellular polymeric substances (EPS) containing polysaccharides,

proteins and lipids (Flemming and Wingender, 2010). In some cases, the formation of biofilms is essential for successful root colonization (Flemming et al., 2016; Meneses et al., 2011).

Here, we describe a novel approach in which rice plants were genetically modified to increase the production of compounds that stimulate the formation of biofilms in diazotrophic bacteria in the soil and promote the bacterial colonization of plant tissues, improving BNF in rice. We first performed a chemical screening to identify compounds that induce biofilm formation in *Gluconacetobacter diazotrophicus* and demonstrated that apigenin and other flavones induced bacterial biofilm synthesis and BNF. We then used CRISPR-based gene editing to modify a flavone biosynthetic pathway in rice, generating apigenin-enriched rice plants that extruded apigenin into the rhizosphere. At limiting soil nitrogen conditions, the increased biofilm production resulted in increased BNF and increased grain yield. Biofilm production also modified the root microbiome structure with enrichment of diazotrophic bacteria recruitment inside the roots and in the rhizoplane and rhizosphere, and increased grain yield under limited nitrogen soil conditions.

Results

A chemical screening for the identification of compounds promoting bacterial biofilm formation

The nitrogen-fixing bacterium *Gluconacetobacter diazotrophicus* was used to develop a high-throughput screening for compounds able to induce biofilm formation (Figure S1a). Bacterial biofilms are clusters of bacteria attached to each other, embedded in a self-produced matrix containing proteins and polysaccharides (Vestby et al., 2020). *Glucanoacetobacter diazotrophicus* was chosen for the screen due to its low background in biofilm staining and the indispensable role of the biofilm in the establishment of mutualistic relationships (Meneses et al., 2011) between the bacterium and the host plants (Cocking et al., 2006). A screen of 740 compounds identified both positive and negative regulators of biofilm production (Figure 1a). The hierarchical clustering of the top 21 positive hits indicated that the majority of them have at least one benzene ring and flavonoids were overrepresented (Backman et al., 2011) (Figure 1b). Secondary tests revealed that 1C08 {N, N′-[(3-Oxo-1-propene-1,3-diyl)di-3,1-phenylene]bis(4-bromobenzamide)}, apigenin and luteolin were the most potent compounds (Figure S1b). Among the top positive hits, the flavones apigenin and luteolin were chosen for further investigation because of (i) their plant origin, (ii) their known role in legume-rhizobium symbiosis (Kent et al., 1986) and (iii) the well-established biosynthesis pathways in rice (Lam et al., 2015). Of the flavone aglycones tested, biofilm formation was only induced by luteolin and apigenin, but not by the upstream naringenin or the downstream chrysoeriol (Figure 1c and d). Flavones are often stored in plants as the more stable forms of glycosides; therefore, the effects of two apigenin glucosides on biofilm formation were also tested; apigenin-7-O-glucoside displayed a positive effect while apigenin-6-C-glucoside (isovitexin) had no effect on biofilm formation (Figure 2a). The biofilm of other diazotrophs including *Azoarcus communis*, *Burkholderia vietnamensis* and *Azospirillum brasilense* could be induced by apigenin or apigenin-7-O-glucoside, which is similar to the response of *Gluconacetobacter diazotrophicus* (Figure 2a). We assessed biofilm formation in the presence of apigenin or apigenin-7-O-glucoside using Confocal microscopy. GFP driven by the *gumD* promoter, a marker for EPS

biofilm matrix (Meneses et al., 2011), was introduced into *Gluconacetobacter diazotrophicus* constitutively expressing mCherry (genpro::mCherry). The high expression of gumDpro:: GFP seen in apigenin- or apigenin-7-O-glucoside-treated bacteria (Figure 2b) indicated an enhanced matrix and biofilm formation, confirming the screening of compounds inducing biofilm formation as reported by crystal violet quantification. The chemically induced biofilm formation favoured biological nitrogen fixation. Both apigenin- and apigenin-7-O-glucoside-treated *Gluconacetobacter diazotrophicus* displayed higher nitrogen-fixing activity than DMSO-treated controls (Figure 2c).

Generation of apigenin-enriched rice lines by CRISPR

The phenylpropanoid biosynthesis pathway generates numerous plant secondary metabolites and contributes to almost every aspect of plant responses (Vogt, 2010). The engineering of plants enriched in chosen flavonoids has long been a goal in agriculture and horticulture (Zhu et al., 2017). Given the effects displayed by both apigenin and luteolin on biofilm formation (Figure 1c and d), the genes encoding O-methyltransferases, mediating the conversion of luteolin to chrysoeriol, would be good candidates to knockout for the generation of plants that could stimulate biofilm production in nitrogen-fixing bacteria. However, the rice genome possesses a large gene family encoding O-methyltransferases, and the knockout of the most abundant member of this family, *ROMT9* (Os08g06100), only slightly increased the total levels of luteolin (Lam et al., 2015). On the contrary, rice has only two genes encoding flavonoid 3′-hydroxylases, CYP75B3 and CYP75B4, that mediate the conversion of apigenin to luteolin (Lam et al., 2015). Since apigenin-7-O-glucoside was more effective than the apigenin aglycone inducing biofilm production (Figure 2), rice flavone glucosyltransferases such as OsUGT707A2 and OsUGT706D1 were not targeted (Peng et al., 2017). CRISPR (Clustered Regularly Interspaced Short Palindromic Repeats) sgRNAs, simultaneously targeting both *CYP75B3* and *CYP75B4*, were designed and transformed into Kitaake rice (Figure 3a). The CRISPR construct comprised a total of 3 sgRNAs targeting *CYP75B3* and *CYP75B4* simultaneously (Methods, Table S3). Sequencing of the transformed *crispr* progenies revealed several lines with mutations in the targeted regions of the genome. For instance, both *crispr* #85 and *crispr* #87 had a truncated *CYP75B3* with a premature stop codon at +493 bp, and a truncated *CYP75B4* with a premature stop codon at +487 bp (Figure 3b). The third allele *crispr* #104 had a frame-shifted, truncated *CYP75B3* with a premature stop codon at +736 bp, and a truncated *CYP75B4* with a premature stop codon at +487 bp (Figure 3a and b). qPCR confirmed that the *crispr* lines displayed little transcripts of both *CYP75B3* and *CYP75B4* (Figure 3c).

The *crispr* rice lines extruded more apigenin, promoted biofilm formation in *Gluconacetobacter*, displayed enhanced biological nitrogen fixation *in vivo* and increased seed yield

Root extracts and root exudates of the *crispr* rice lines contained significantly higher amounts of apigenin than those from Kitaake control plants (Figure 3d and e). In root extracts, the apigenin aglycone was more abundant than the apigenin-7-O-glucoside (Figure 3d). However, the ratio between apigenin aglycone and its glycosides fluctuated in the exudates, likely due to the complex enzymatic reactions at the microbiota in the rhizosphere (Hartwig and Phillips, 1991) and the action of microbial glycosidases (Hyung Ko et al., 2006; Meech et al., 2019). The extracts from
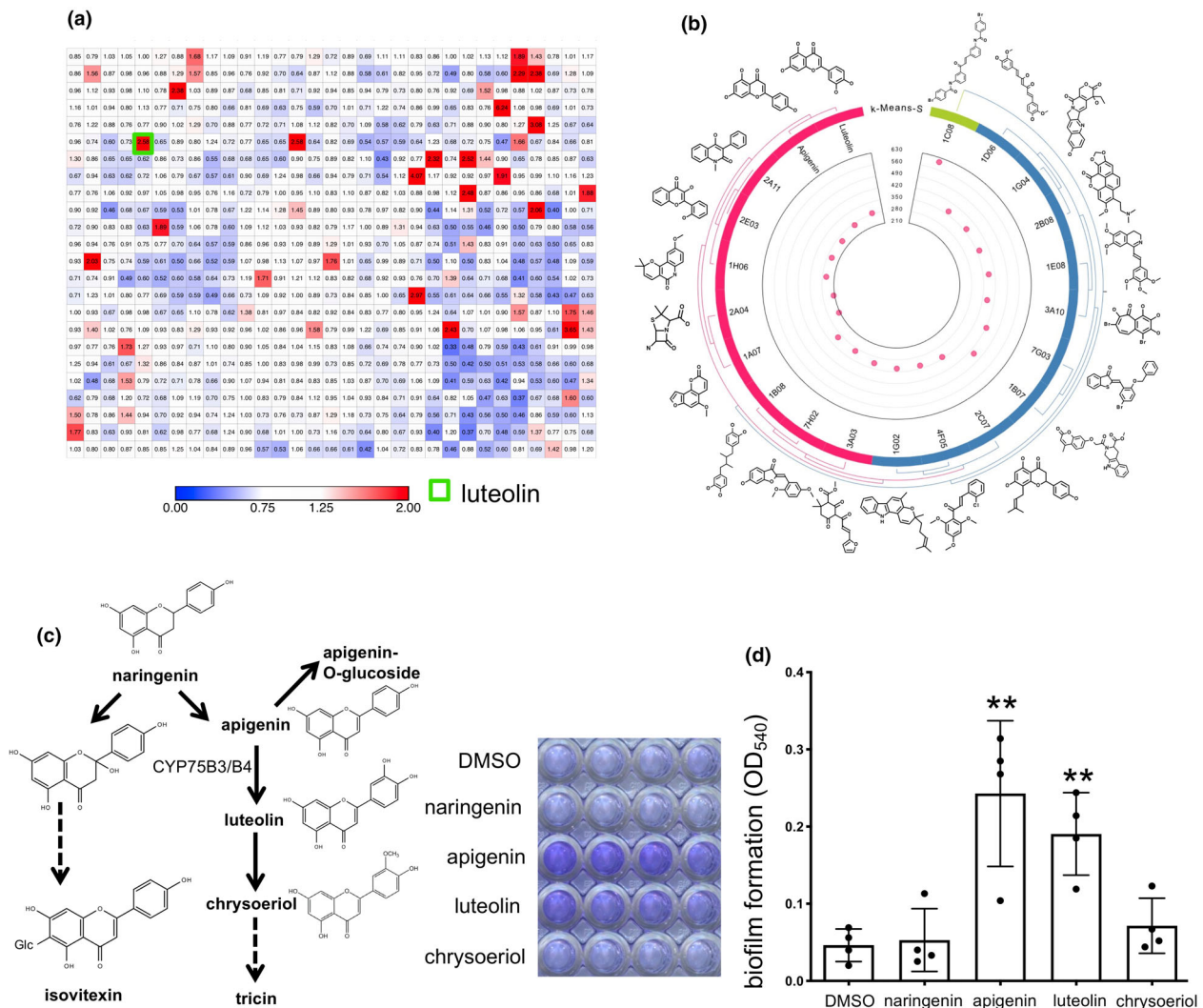
Figure 1 Chemical screening identifies apigenin and luteolin as biofilm inducers for the nitrogen-fixing bacteria *Gluconacetobacter diazotrophicus*. (a) Chemical screening was performed in the 96-well plate with each well containing: 198 μL of the Kitaake roots exudate and 2 μL of the 10 mM compound from the chemical libraries. Equal volume (2 μL) of DMSO was added to the well and served as the negative control. *Gluconacetobacter diazotrophicus* was added to the final OD600 = 0.01 to each well and incubated in a shaker at 150 rpm, 28 °C for 3 day before biofilm quantification by crystal violet staining. The value of each well in biofilm quantification was normalized to that of the DMSO control in each plate (DMSO = 1). The heatmap was generated by the mean value of 3 biological replicates for each compound using MORPHEUS software (https://software.broadinstitute.org/morpheus/). (b) Chemical structures and hierarchical clustering of the top 21 positive regulators of biofilm based on pairwise compound similarities defined using the Atom Pair descriptors and Tanimoto coefficiency (http://chemmine.ucr.edu/). The chemicals are also clustered into three groups with different colours by the K-Means algorithm. Pink dots in the inner cycles represent molecular weight of each compound. (c) Key intermediates in the flavone biosynthetic pathway and their chemical structures. (d) Flavone-induced biofilm formation in *Gluconacetobacter diaztrophicus*. Values are the Mean ± SD (*n* = 4). **P < 0.01 (One-way ANOVA followed by Dunnett's test compared with DMSO control).

the *crispr* plants induced more biofilm formation of *Gluconacetobacter diazotrophicus* than the Kitaake extracts (Figure 4a). It should be noted that although the effects of root extracts on bacteria biofilm formation varied between different preparations, the biofilm formation induced by extracts from the *crispr* lines was always higher than that from extracts from Kitaake control plants. Similar results were obtained with root exudates (Figure 4b). These results were confirmed *in vivo*. Root of the rice *crispr* plants induced higher *gumDpro*::GFP expression in *Gluconacetobacter diazotrophicus* than that from Kitaake plants (arrows in Figure 4c), indicating the enhanced transcription of

gumD, encoding exopolysaccharide (EPS), critical to biofilm formation. To assess whether the enhanced biofilm production induced by the root exudates promoted nitrogen-fixing activity in the bacteria associated with the roots, we measured the assimilation of ^{15}N-dinitrogen gas into roots by isotope ratio mass spectrometry (IRMS). ^{15}N-assimilation was measured *in vivo* at two rice developmental stages: at panicle formation and mature plants in 8-week-old and 16-week-old plants, respectively (Figure 4d). Rice *crispr* plants displayed a large increase in ^{15}N content at both developmental stages, indicating the increased ^{15}N$_2$ fixed to ammonia by the soil bacteria and its assimilation by
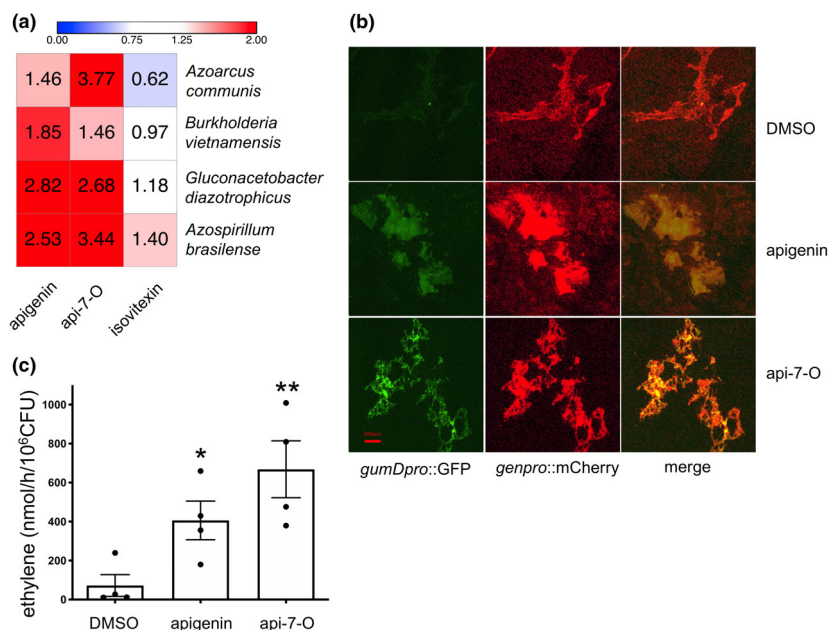
Figure 2 Apigenin and apigenin-O-glucoside induce biofilm and promote nitrogen fixation *in vitro*. (a) Biofilm formation of various nitrogen-fixing bacteria in the presence of apigenin aglycone, apigenin-7-O-glucoside (api-7-O) or apigenin-6-C-glucoside (isovitexin) using crystal violet staining. The value of each well was normalized to that of the DMSO control for each bacteria (DMSO = 1). The heatmap was generated using the Mean of 5 biological replicates using MORPHEUS software (https://software.broadinstitute.org/morpheus/). (b) The apigenin aglycone and apigenin-7-O-glucoside induced the expression of the *gumD* gene, which is responsible for the first step in exopolysaccharide (EPS) production of biofilm in *Gluconacetobacter diazotrophicus*. The *Gluconacetobacter diazotrophicus* was double labelled with a constitutive expressed mCherry (*genpro*::mCherry) and the promoter of the *gumD* gene driving GFP (*gumDpro*::GFP). The double labelled bacteria was cultured the same way as the biofilm quantification in the presence of apigenin, and observed by Confocal microscope. (c) The apigenin aglycone- and apigenin-7-O-glucoside-treated *Gluconacetobacter diazotrophicus* promotes nitrogen fixation as demonstrated by acetylene reduction assay (ARA). Data are the Mean ± SEM ($n = 4$). *$P < 0.01$ and **$P < 0.05$ (One-way ANOVA followed by Dunnett's test compared with DMSO control).

the rice plants. The relatively lower amount of ^{15}N assimilated by roots from mature plants (Figure 4d) was probably due to the known decrease in N assimilation by mature plants, where most of the N in the grain is derived largely from mature organs (leaves and stems) by degradation of chloroplastic proteins (Yoneyama et al., 2016).

Our results showed that the high apigenin and apigenin derivatives extruded by the *crispr* rice plants induced increased biofilm formation in soil bacteria (Figures 2 and 3). This process has particular relevance in soil associative nitrogen-fixing bacteria, where the biofilm contributes to the maintenance of low oxygen conditions, thus facilitating nitrogenase activity and the fixation of nitrogen from the atmosphere (Oelze and Klein, 1996). In order to evaluate whether biological nitrogen fixation contributed to N-assimilation by the rice plants, Kitaake and *crispr* plants were grown under control (75 ppm N) and limiting (22.5 ppm N) nitrogen conditions (Figure 5). No significative difference between agronomic traits were seen between Kitaake and the *crispr* rice lines (Figure S2). The higher chlorophyll b and total chlorophyll contents in the *crispr* lines suggested a lesser effect of N-deficiency (Figures S2j, k and l). At the maturing stage, all *crispr* lines displayed a shorter phenotype (Figure 5a and b), an increased panicle number (Figure 5a and c) and a 20%–35% increased seed yield (Figure 5d). Most importantly, the *crispr* lines had equal or higher level of the total nitrogen content per gram of seeds (Figure S3f), resulting in higher nitrogen per plant (Figure S3g). Overall, the above results showed that the *cripsr* plants

assimilate and translocate the fixed nitrogen to the sink. Plants grown under control conditions did not show differences in panicle number or seed yield (Figure S3).

Apigenin-enriched rice recruited a distinct microbiota towards biological nitrogen fixation

Apigenin and apigenin-7-O-glucoside promoted biofilm formation in several known nitrogen-fixing bacteria (Figure 2a). Bacteria that were associated with the roots of *cripsr* plants were tested for biofilm formation in the presence of apigenin. Eighty colonies grown on Jensen's N-free medium (Jensen, 1942) (capable of using atmospheric nitrogen gas as the only N source) were tested (Figure S4a). As compared to the controls, 42.5% (34 out of 80) and 67.5% (54 out of 80) of the colonies produced more biofilm in the presence of apigenin. Some of the bacteria was identified by 16S sequencing (Figure S4a).

We assessed whether the extruded apigenin in the *crispr* plants affected the root microbiota. Rice *crispr* line #87 plants grown in 'Veggie-Mix' soil displayed a 35% increase in yield as compared to Kitaake grown under limiting N conditions (Figure S3e), similar to plants grown in '80% sand/20%peat mix' soil (Figure 5). Two months after plants were transplanted to soil, root rhizosphere, rhizoplane and endosphere were separated and 100 samples were collected, including the unplanted bulk soil grown at the same conditions, for 16S bacterial profiling. Principal coordinates analysis (PCoA), measured by Bray–Curtis distance, was used to visualize the samples, and 27 samples that deviated from the gradual transition of bacterial composition from soil to
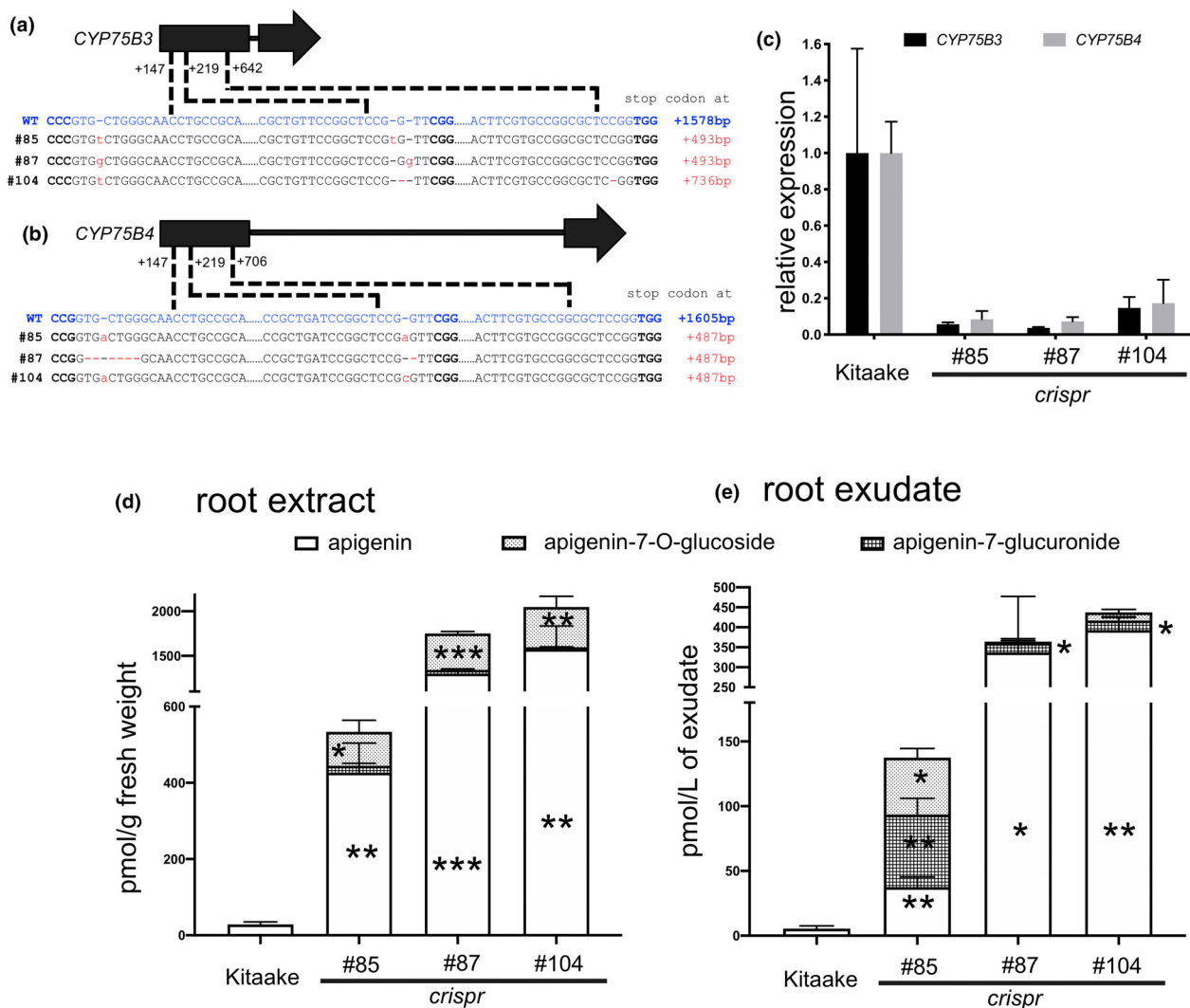
Figure 3 CYP75B3/CYP75B4 knockout plants accumulate apigenin in roots and root exudates. (a), (b) Gene structure and the three sgRNA targeting sites for CYP75B3 (a) and CYP75B4 (b). Wild type sequences for the targeting sites are highlighted in blue while the CRISPR-modified sequences are highlighted in red. The PAM sequences (NGG or CCN) are highlighted in bold. The same mutations were verified in both T1 and T2 generations. (c) The *crispr* plants showed little expression of the targeted genes as measured by qRT-PCR. Similar expression levels were obtained in both T1 and T2 generations. RNA was sampled from leaves, and primers were listed in Table S3. Data presented from here were obtained from T2 generation (refer to *crispr* hereinafter). (d), (e) Both the aglycone and the O-glucoside of apigenin were enriched in the root extracts (d) and root exudates (e) of the *crispr* lines. Data are the Mean $\pm$ SEM ($n = 4$ for root extract, $n = 5$ for root exudate). *$P < 0.05$, **$P < 0.01$ and ***$P < 0.001$ (Two-sided Student's *t*-test compared with Kitaake control).

rhizosphere, rhizoplane and endosphere were removed from further functional analysis (Methods, Figure S4b).

For the alpha diversity, the richness of bacterial actual sequence variants (ASV) (representing the number of species or strains, within a single sample) decreased closer to the root, regardless of the plant genotype (Figure 6a), indicating an expected strong selection by the host plant. The Wilcoxon rank test indicated no significant differences in ASV richness between Kitaake and the *crispr* line in all root compartments tested (Figure 6a). On the contrary, the beta diversity measured by PCoA demonstrated that the plant genotype played a significant role in shaping the microbiota. As expected, bulk soil, rhizosphere, rhizoplane and endosphere samples separated from each other, indicating their differences (Figure 6b). Most importantly, principal coordinates analysis (PCOA) measured by Bray–Curtis distance revealed that microbiota recruited by the *crispr* plants clustered separately from

the Kitaake control plants in all three compartments: rhizosphere, rhizoplane and endosphere (Figure 6c). When the significance of the compartment and the genotype in the composition of the bacterial community was considered in a PerMANOVA (Figure 6b and c), both factors were significant at $P < 0.001$, (Compartment $F_{3,66} = 18.63$; Genotype $F_{1,66} = 4.76$) without significant interaction ($F_{2,66} = 1.01$; $P = 0.36$).

Sequence libraries consisted of bacteria from 43 phyla (Figure S5a), with the most abundant phyla comprising Proteobacteria (63.1%), Bacteriodota (9.4%) and Myxococcota (5.3%). Of the 423 total bacterial genera classified across the experiment, the abundance of 7 genera had a higher abundance in one or more compartments associated with the *crispr* plant genotype, while 11 genera had a significantly lower abundance relative to the Kitaake genotype (Figure 6d). Similar analysis at the order and family levels are presented in Figure S5b and c.
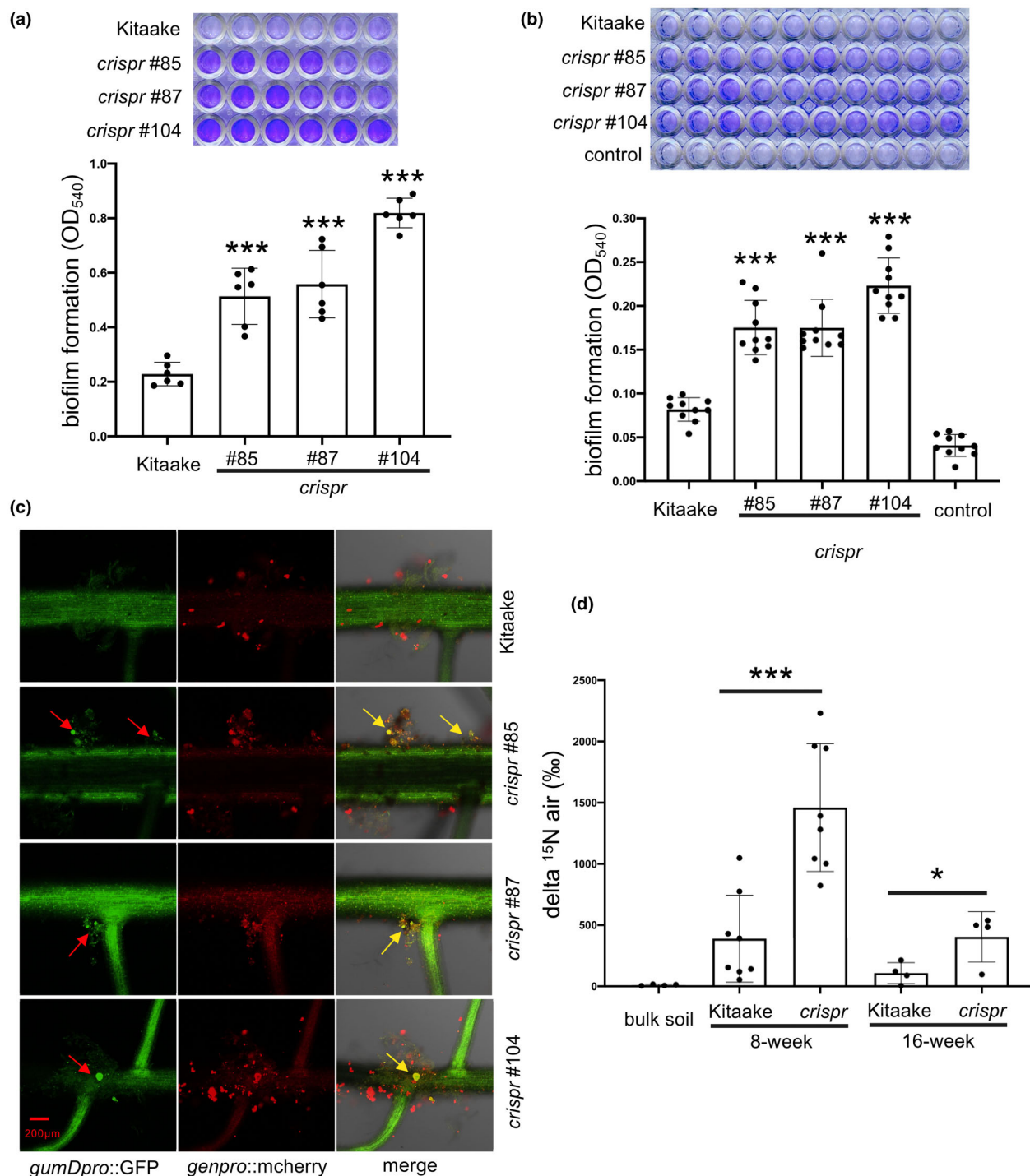
Figure 4 *crispr* lines induce more biofilm and fix more nitrogen. (a), (b) Whole-plant extracts (a) and root exudates (b) of the *crispr* lines generate more biofilm in *Gluconacetobacter diazotrophicus* as assessed by crystal violet staining. Biofilm quantification was performed after 4 days of growth, Values are the Mean $\pm$ SD ($n = 9$ for a, $n = 10$ for b). Control in (b) represents 1% sucrose and 1% mannitol without any root exudates. ***$P < 0.001$ (One-way ANOVA followed by Dunnett's test compared with Kitaake control). (c) The root of the *crispr* lines induced higher expression of the *gumD* gene in *Gluconacetobacter diazotrophicus*. The seven-day-old plants were inoculated by the double labelled bacteria (*genpro*::mcherry and *gumDpro*::GFP), and grown hydroponically in 22.5 ppm N for 30 days prior to Confocal analysis. Red arrows: *gumDpro*::GFP signal for biofilm. Yellow arrows: yellow signal results from the merge of GFP and mCherry. (d) The *crispr* line #87 incorporated more nitrogen from the air (delta ^{15}N) when grown in the greenhouse at both 8 weeks and 16 weeks after transplanting. *$P < 0.05$ and ***$P < 0.001$ (Two-sided Student's *t*-test compared with Kitaake control).

Since apigenin induced biofilm formation in various nitrogen-fixing bacteria (Figures S2a and S4a) and the apigenin-enriched *crispr* plants displayed a higher BNF activity (Figure 4d), we focused on the nitrogen-fixing bacteria in the metagenomic data. When looking at the impact of plant genotype on the presence or abundance of predicted nitrogen-fixing bacteria based on
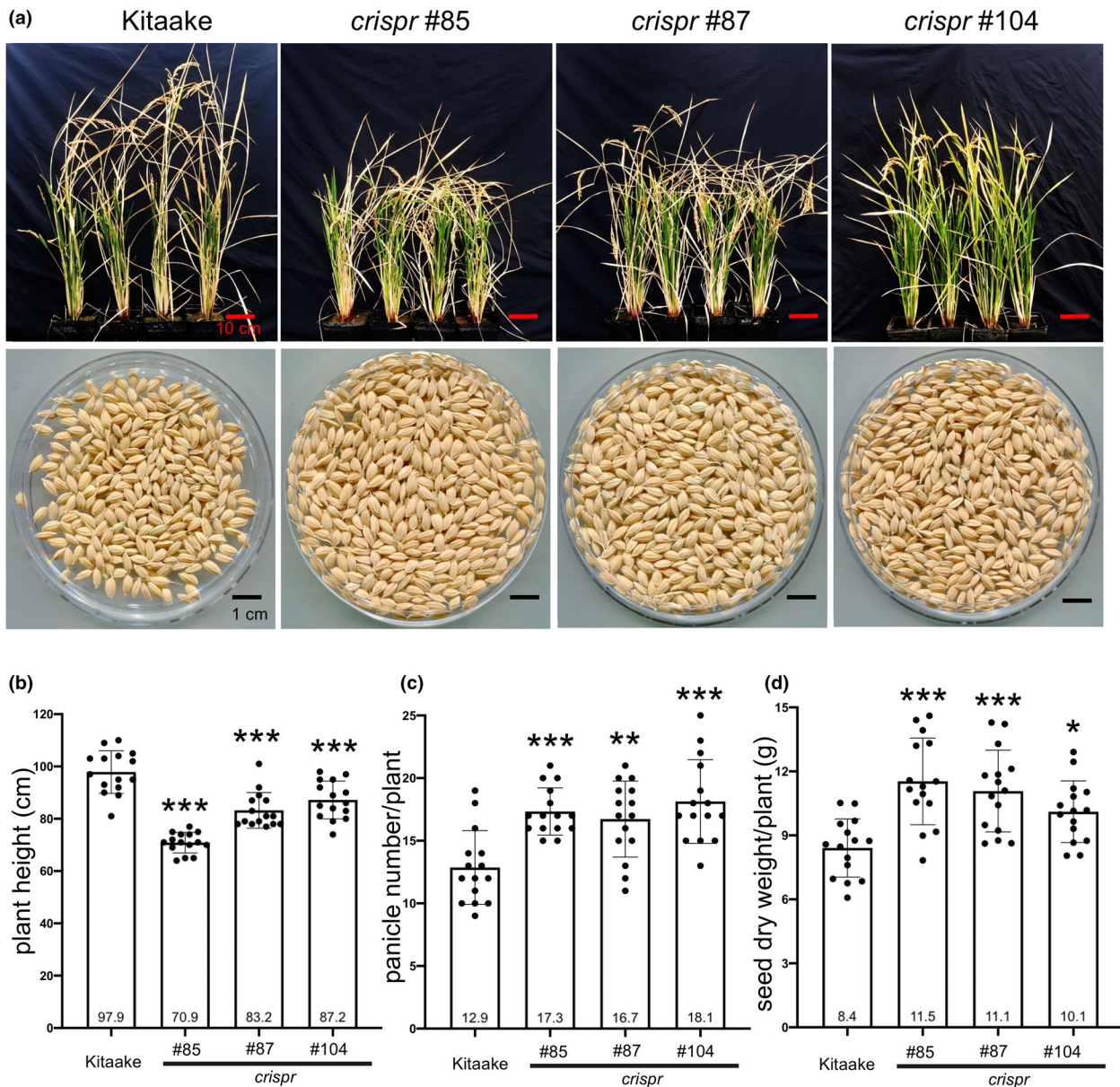
Figure 5 *crispr* lines produced more seeds under nitrogen-limited conditions. (a) The morphology of 16-week-old rice grown in 30% nitrogen medium. (b)-(d) The *crispr* lines have reduced plant height (b) increased panicle numbers (c) and higher dry weight of seeds (d). Data are the Mean ± SD (*n* = 15). *P < 0.05, **P < 0.01 and ***P < 0.001 (One-way ANOVA followed by Dunnett's test compared with Kitaake control).

FAPROTAX classification (Louca *et al*., 2016), we first modelled the presence–absence of putative nitrogen-fixing bacteria across treatments in a two-way ANOVA analysis where compartment and genotype were included as factors. Plant genotype was a significant factor ($F_{1,64}$ = 23.0; P < 0.0001) modelling the richness of predicted nitrogen-fixing bacteria, and the *crispr* plants showed significantly higher nitrogen-fixing bacteria ASV richness across all three root compartments than that in the control plants (Figure 6e, Figure S6a). The Wilcoxon rank tests indicated that the proportion of putative endosphere nitrogen-fixing bacteria in the *crispr* plants was significantly higher (W = 175, P = 0.030), with an average of 0.85% in the *crispr* genotype and 0.66% in the Kitaake genotype (Figure S6b). There were no significant differences in the nitrogen-fixing bacteria relative abundance

between plant genotypes in the rhizoplane (W = 132, P = 0.43) or the rhizosphere (W = 6, P = 0.41).

Discussion

The induction of soil bacterial biofilm formation by plant exudates and the generation of microaerophilic conditions could increase the nitrogen fixation activity of the diazotrophic bacteria in the soil, providing ammonia to plants. We applied a chemical screening approach and designed a functional screen of natural and synthetic compounds targeting bacterial biofilm formation, an imperative process for both bacteria's success in colonizing plants and efficient nitrogen fixation. The identification of plant-synthesized compounds and the modification of their
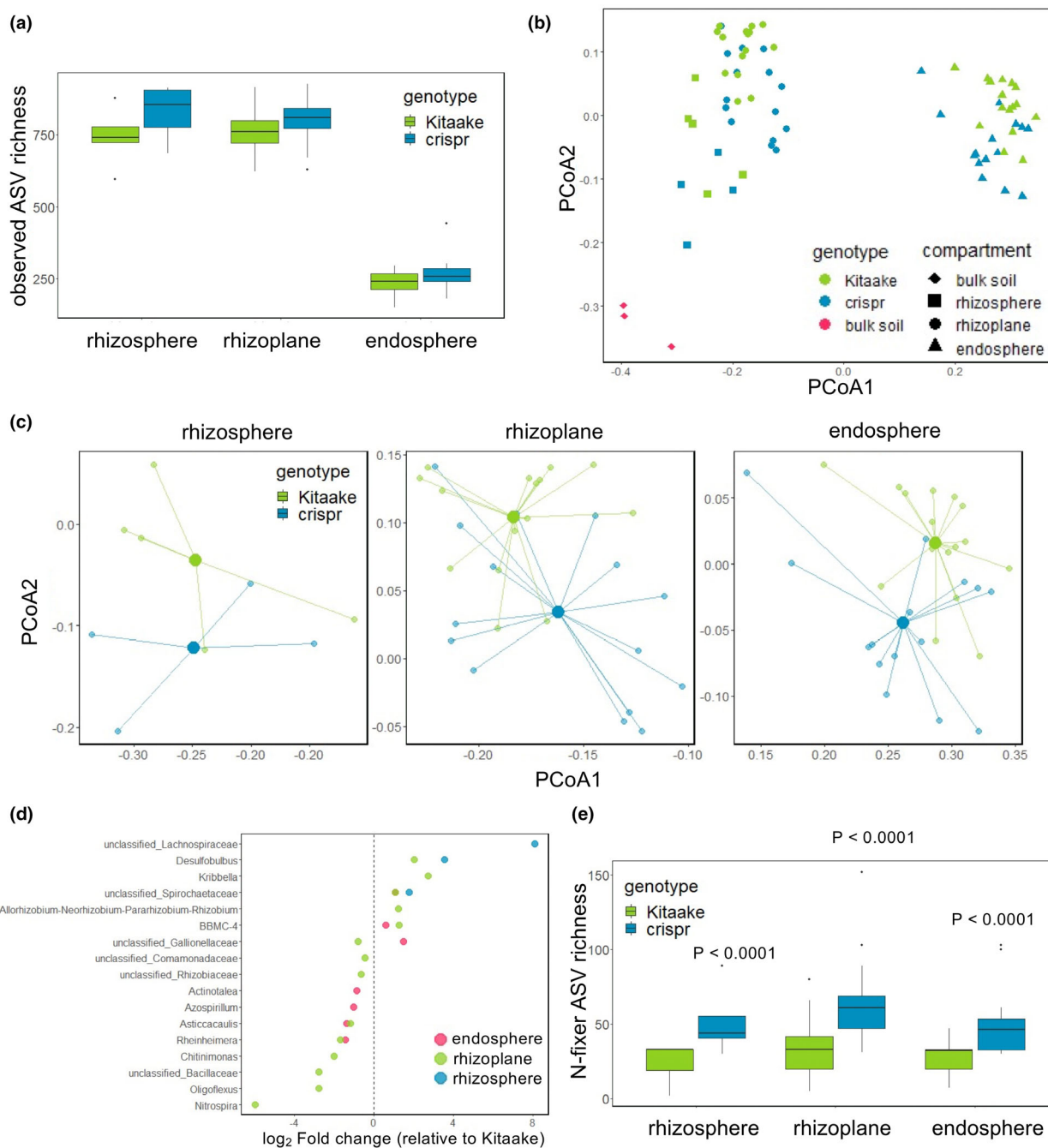
Figure 6 *crispr* line recruits a distinct microbiota towards biological nitrogen fixation. (a) Alpha diversity as measured by the Observed Richness of bacterial actual sequence variants (ASV) in the rhizosphere, rhizoplane and endosphere between Kitaake and *crispr* line. (b), (c) The *crispr* line recruits a distinct microbiota in the rhizosphere, rhizoplane and endosphere. Principal coordinate axes (PCOA) of bacterial ASV composition across root compartment and genotype. Centroids of Bray–Curtis dissimilarity scores for the composition of all three root compartments in the *crispr* differed from Kitaake control. Centroids were calculated from the mean PCOA 1 and 2, visualized as the large centre dots connected to each data point from a treatment (c). (d) Genera with a significantly different abundance in the *crispr* line relative to Kitaake across the three plant compartments. (e) The observed richness of nitrogen-fixing bacterial ASV predicted by FAPROTAX were significantly higher in all three compartments in the *crispr* line than that in the Kitaake. ($F_{1,64}$ = 23.0; $P < 0.0001$) two-way ANOVA. Neither plant compartment ($F_{2,64}$ = 1.8; $P = 0.17$) nor the interaction between genotype and compartment ($F_{1,64}$ = 0.34; $P = 0.71$) were significant. For the whisker plot in (a) and (e) the horizontal bars within boxes represent medians. The tops and bottoms of boxes represent the 75th and 25th percentiles, respectively. The upper and lower whiskers extend to data no more than 1.5× the interquartile range from the upper edge and lower edge of the box, respectively. The outliers are shown as dots.

biosynthetic/degradation pathways would enable the accumulation of the compound of interest in the plant roots and its release into the rhizosphere.

Several flavonoid compounds that increased biofilm formation in the nitrogen-fixing bacterium *Gluconacetobacter diazotrophicus* were identified (Figure 1). Flavonoids are released by plant

roots into the rhizosphere and play different roles associated with the control of plant–soil interactions (Cesco et al., 2012). Flavonoids have been used by plants for adaptation to new environments since liverworts and mosses first colonized land (Rausher, 2006). Flavonoid compounds are critical to the symbiosis between legumes and rhizobia, inducing rhizobial Nod genes which signal for nodule formation (Zhang et al., 2009) and chemotaxis (Hartwig et al., 1991). Apigenin and 7,4'-dihydroxyflavone are among the most potent inducers of the Nod genes and have been shown to accumulate in root border cells released from the root cap (Watson et al., 2015). Unlike the well-documented roles of flavones in legume-rhizobia symbiosis, little is known about the effect of flavones on the interaction between bacteria and cereal crops. In maize, the inbred line 787 has been shown to increase the expression of flavone synthase and to extrude ~5 times more apigenin and luteolin, promoting the enrichment of Oxalobacteraceae in the rhizosphere and improving plant performance under nitrogen-limited conditions (Yu et al., 2021). The effects of apigenin on biofilm production of several diazotrophic bacteria varied with species but was stimulatory in all cases, suggesting that apigenin could act as a general stimulant for biofilm formation in nitrogen-fixing bacteria (Figure 2a). The formation of the biofilm EPS creates heterogeneity, including the establishment of stable gradients of nutrients and redox conditions, critical to nitrogenase function (Flemming et al., 2016). Biofilms enabled free-living Pseudomonas stutzeri A1501 and Azospirillum brasilense to fix nitrogen under natural aerobic conditions (Wang et al., 2017), and biofilm production in Gluconacetobacter diazotrophicus was correlated with increased nitrogen-fixing activity (Figure 2c).

We anticipated that rice apigenin contents and the apigenin extruded by the roots could be increased by inhibiting apigenin catabolism. We applied CRISPR/Cas9 methodology to knockout CYP75B3 and CYP75B4, encoding flavonoid 3'-hydroxylases that mediate the conversion of apigenin to luteolin in Kitaake rice plants (Figure 3a, b and c), increasing apigenin and apigenin O-glucoside contents in crispr root extracts and exudates (Figure 3d). Flavonoid glycosides are rapidly hydrolysed by both plant and microbial glycosidases (Hartwig and Phillips, 1991). The engineering of apigenin catabolism lead to the decrease of other flavones such as tricin (Lam et al., 2019). Whether alteration in the flavones profiles changes the susceptibility of the plants to withstand bacterial or fungal infections requires further investigation.

The apigenin concentrations required for the detection of biofilm induction in vitro (Figure S1b) were larger the concentrations those that were effective in inducing biofilm formation and nitrogen fixation in vivo (Figure 4). A number of factors could explain these differences: (i) in vitro measurements were made after 2-day period, while the crispr plants extruded apigenin continuously, (ii) apigenin could accumulate at a much higher concentration on the root surface in a spatial–temporal pattern, (iii) apigenin solubility, (iv) other metabolites in the root exudates may also contribute to bacterial biofilm formation, etc. The role of apigenin in biofilm formation in the root compartments of the crispr rice plants and BNF induction was further supported by a 20%–35% yield increase when the plants were grown under limiting N conditions (Figure 5). Plant height reduction, observed at both control and limiting N conditions, might be related to flavonoid-induced changes in lignin homeostasis (Figures 5b and S2a; Lam et al., 2019). A rice mutant of FLAVONE SYNTHASE II encoding CYP93G1 that catalyses the conversion of naringenin to apigenin also displayed a shorter plant phenotype (Lam et al., 2017), suggesting that the height

phenotype displayed by the crispr lines was not the consequence of apigenin accumulation. The cripsr line grown under control condition (75 ppm) displayed similar phenotype showed no increase in yield (Figure S3), suggesting that the yield gain under limiting nitrogen condition (25 ppm) is not related to the shoot height phenotype. Reduced plant height and increased tillering are associated with increased grain yield (Liu et al., 2018). Although the reduction in height of the crispr plants needs more research, shorter plants with higher grain yield would have a higher harvest index, consuming less water and other resources. These characteristics were an important drive of the 'Green Revolution' (Khush, 2001). However, Green Revolution varieties are often associated with reduced nitrogen use efficiency (Li et al., 2018). The crispr rice lines, growing at limiting nitrogen conditions, displayed reduced height, increased tiller number and increased grain yield (Figure 5).

Our results indicated that apigenin catabolism had limited effects on the alpha diversity of the root microbiota, since the bacterial variant richness was similar in Kitaake and crispr root compartments. However, the crispr plant roots recruited a distinct microbiota with higher nitrogen-fixing bacteria in the root rhizosphere, rhizoplane and endosphere than the Kitaake roots (Figure 6). Since soil microbiome is greatly affected by environmental cues and soil habitat-related factors, the similar results obtained in two very different soils 'Veggie Mix' and '80%sand/20%peat mix' indicated that crispr plants have a strong adaptability to the environment.

Inoculation of nitrogen-fixing bacteria such as Azoarcus, Azospirillum and Burkholderia has limited success in the field, partially because the inoculants were outcompeted by native microbial communities in the rhizosphere of plants (Rosenblueth et al., 2018). Rather than improving the surviving rate and activity of certain bacteria for inoculation, our work presents a new avenue of generating a better host for the indigenous nitrogen-fixing bacteria (Figure 6e) by inducing their biofilm (Figure S4a), which is critical for surviving, colonizing the host and protecting nitrogenase activity. In contrast to the promoting effect on biofilm formation in nitrogen-fixing bacteria, plant polyphenols (including apigenin) are well known for their antibiofilm functions in pathogenic bacteria (Slobodníková et al., 2016). It is possible that the apigenin-enriched microenvironment generated by the cripsr line selectively induces biofilm of soil diazotrophs, increasing their ability to colonize host plants.

In conclusion, our results indicate that the manipulation of the flavone biosynthetic pathway, with the concomitant increase in root exudate flavone contents, provides a general strategy to induce biofilm formation in soil diazotrophs under limiting nitrogen and aerobic conditions. The formation of biofilm protects the bacterial nitrogenase and promots root–diazotroph interaction and root colonization, resulting in efficient biological nitrogen fixation. Flavonoid synthesis in general, flavonoid 3'-hydroxylases in particular, is ubiquitously distributed among cereals (Figure 6; Wen et al., 2020). Thus, our results support the manipulation of the flavone biosynthetic pathway as a feasible and general strategy for the induction of biological nitrogen fixation in cereals through biofilm formation in soil diazotrophs.

Methods

Plant growth conditions

Rice seeds were dehusked and surface-sterilized in a diluted bleach solution (2% sodium hypochlorite and 0.05% Tween 20)

for 10 min and rinsed 5 times in sterile milli-Q water. The sterilized rice seeds were then germinated in the dark for 5 days at 28 °C before being placed in Yoshida solution (Yoshida et al., 1976) for 7 day at 16 h light/8 h dark at 28 °C and transplanted to soil. The soil 'Veggie Mix' was purchased from Hastie's Capitol Sand and Gravel (Sacramento, CA) and has the following composition: 25% screened topsoil, 5% lava fines and sand and 70% of equal parts of Forest humus, organic compost and mushroom compost. The soil '80% sand/20%peat mix' was homemade at UC Davis and used for culturing rice. Both soils were analysed at UC Davis analytical laboratory (Table S1). Rice medium with different nitrogen concentrations (100%, 75 ppm N and 30%, 22.5 ppm N) was provided through the Tefen MixRite 2.5 injector from two concentrated fertilizer tanks in the 0.5% injection ratio (Table S2). Rice medium was added to a tub containing 10 square pots (size 6″ × 6″) twice a week or as needed.

Bacteria and biofilm screening assay

Gluconacetobacter diazotrophicus (ATCC, 49037), *Azoarcus communis* (ATCC, 51397) and *Burkholderia vietnamiensis* (ATCC, BAA-248) were obtained from American Type Culture Collection (Manassas, VA). *Azospirillum brasilense* was provided by Dr. Igor B. Zhulin (Wisniewski-Dyé et al., 2011).The biofilm assay was performed as previously described (Genevaux et al., 1996) with some modifications. Briefly, *Gluconacetobacter diazotrophicus* cultures were grown overnight in a modified ATCC medium (0.5% yeast extract, 0.3% peptone, 1.5% sucrose and 1.5% mannitol) at 28 °C. The cultures were diluted at 1 : 50 in fresh ATCC medium, and cultures were grown to $OD_{600} = 0.4$. The cultures were pelleted, and the supernatant was discarded. The pellets were washed 3 times with sterile water and then suspended with exudates from 3-day-old Kitaake germinating seedlings to a final $OD_{600} = 0.01$. The exudates used for biofilm assays were collected by germinating 50 Kitaake seeds in 25 mL of sterile milli-Q water for 3 day at 28 °C in the dark. Two μL of the compound (10 mM) from the indicated chemical library was added to 198 μL of bacteria plus Kitaake exudates in each well of a sterile 96-well plate (Corning 3595), resulting in a final concentration of 100 μM of each compound. The 96-well plates were shaken (150 rpm at 28 °C) for 3 day. After incubation, the planktonic cells were discarded. Two hundred μL of crystal violet solution (0.2% crystal violet, 2% ethanol in water) was added to each plate well, and the plates were shaken at 28 °C (150 rpm for 30 min). The solution in each well was discarded, and the plates were rinsed 3–4 times with water and air-dried. Two hundred μL of 95% ethanol was added to each well to solubilize the crystal violet and shaken at 28 °C (150 rpm for 15 min), and the absorbance was measured at 540 nm (Biotek Synergy Mx plate reader). The chemical libraries used are Flavonoid derivatives collection FL-500 (TimTec) and Greenpharma Natural Compound Library (Prestwick Chemical). Naringenin (N5893), apigenin (10798), luteolin (L9283), isovitexin (17804) and apigenin-7-O-glucoside (44692) were purchased from Sigma-Aldrich (St. Louis, MO).

Confocal microscopy

The *genpro*::mCherry and *gumDpro*::GFP labelled *Gluconacetobacter diazotrophicus* was cultured in the presence of 100 μM apigenin, apigenin-7-O-glucoside or DMSO or in the presence of exudates of the *crispr* or Kitaake for the indicated times. Thirty μL of the culture was added to the 24 × 60 mm cover slide and visualized with a Zeiss LSM 710 laser scanning Confocal system using standard GFP and mCherry settings. For the biofilm observation on the rice root, seven-day-old *crispr* or Kitaake plants were inoculated by the *genpro*::mCherry and *gumDpro*:: GFP labelled *Gluconacetobacter diazotrophicus* to the final OD600 = 0.02 and grown hydroponically at 22.5 ppm N medium for 30 days prior to Confocal imaging.

Acetylene reduction assay

Gluconacetobacter diazotrophicus was added to a final $OD_{600} = 0.01$ in a tube containing rice exudates with different compounds and was shaken for 3 day at 28 °C for biofilm formation. Ten % of the air in the tube was then replaced by acetylene, and the tube was further incubated in the dark for 3 day before ethylene measurements using a gas chromatograph (Shimadzu CG-8A gas chromatograph, Shimadzu Scientific Instruments, Kyoto, Japan). Ethylene was calculated by plotting the peak area against an ethylene standard curve.

$^{15}N_2$ incorporation assay

A 10 cm segment of the root, around 5 cm below the root–shoot junction, was harvested after shaking off the loosely attached soil and sealed in a 20 mL glass tube. Soil (5 cm deep) from pots without plants but in the same rice medium was sampled as bulk soil control. Ten ml of air in the tube was then replaced with $^{15}N_2$, and the tubes were incubated at 28 °C for 3 day. The roots or bulk soil were taken out of the tube, dried at 60 °C for 7 day before ^{15}N analysis at UC Davis Stable Isotope Facility. The values of the isotope ratio were expressed as delta ^{15}N air (‰), according to the formula delta ^{15}N air (‰) = [(Rsample/Rair) − 1]·1000, where Rsample is $^{15}N/^{14}N$ of the soil or plant material while the Rair used was the N isotope ratio in the atmosphere air (Rair = 0.0036765).

Vector construction and rice transformation

The *genpro*::mCherry construct was assembled by the In-Fusion cloning kit (TakaraBio, San Jose, CA) using the pBBR1 replicon and the gentamycin resistance gene promoter (Ramos et al., 2002), the gentamycin promoter from the pSEVA637 (SEVA, Madrid, Spain) to the PacI and NotI digested pSEVA237R vector (SEVA, Madrid, Spain). For the *gumDpro*::GFP construct, a 496 bp genomic sequence upstream of the *gumD* gene was PCR-amplified from the *Gluconacetobacter diazotrophicus* genome and cloned into the promoterless GFP vector pSEVA637 by KpnI and PacI digestion-ligation cloning. To build the CRISPR/Cas9 vector p250d-CYP75B3B4, 3 target sites (T1; TGCG GCAGGTTGCCCAGCAC, T2; CCGCTGTTCCGGCTCCGGTT and T3; ACTTCGTGCCGGCGCTCCGG) were chosen. T1 and T3 are common to both *CYP75B3* and *CYP75B4* genes while T2 is a perfect match with B3 and 1 nt mismatch with B4. The polycistronic tRNA-gRNA cassette was artificially synthesized (Invitrogen, Waltham, MA) with TaU3 promoter, 35S terminator and AarI sites which are compatible with the downstream GoldenGate cloning step. The sequence of synthesized CYP75 multiplex gRNA cassette is listed in Table S3. The synthesized gRNA cassette, pMOD_A1110 (Addgene # 91031) harbouring TaCas9 and the acceptor vector pTRANS_250d (Čermák et al., 2017) were assembled with AarI GoldenGate reaction. The p250d-CYP75B3B4 was transformed into Kitaake by EHA105 *Agrobacterium* in the Plant Transformation Facility at UC Davis.

Three independent T0 lines (#85, #87 and #104) were propagated to select the homozygous lines. The homozygous lines were confirmed to have the same mutations in T1 and T2 generations. For qPCR, leaf RNA was extracted using Qiagen RNeasy Mini Kit (Qiagen, Redwood City, CA). DNA contamination was removed using the TURBO DNA-free Kit (Thermo Fisher Scientific, Waltham, MA), and the RNA was reverse transcribed using the QuantiTect reverse transcription kit from Qiagen. qRT-PCR was performed in the StepOnePlus Real-Time PCR System using Fast SYBR Green Master Mix (Thermo Fisher Scientific, Waltham, MA). The relative expression of the targeted genes was normalized to the reference genes LOC_Os02g06640, LOC_Os03g13170 and LOC_Os08g03290 (Pabuayon et al., 2016). The primers are listed in Table S3.

Flavonoid measurements in rice extract and root exudates

Seedlings were grown hydroponically in 5-gallon plastic pails containing 22.5 ppm N for 2 months. For exudate collection, each rice plant was rinsed 5 times in sterile milli-Q water and then placed in a light-protective container (one plant per container) with 150 mL of sterile milli-Q water for 2 day. The exudates were collected and filtered through a 0.45 μm Corning 50 mL tube top vacuum filter system and freeze dried. For root extracts, 2-week-old Kitaake and crispr plants grown in 22.5 ppm N were transferred to sterile milli-Q water for 2 day. The roots were harvested, ground into fine powder in liquid nitrogen and dissolved in HPLC grade methanol. Both the root exudates and the root extracts were stored at −80 °C until measurement. Flavonoids were measured in an ultra-performance liquid chromatography—high-resolution mass spectrometry (Thermo Scientific Q Exactive Focus Orbitrap LC—MS/MS System). The parameters were as follows: UPLC: pump, UltiMate 3000 HPG-3400RS; autosampler, UltiMate 3000 WPS-3000PL; Column Compartment: UltiMate 3000 TCC-3000RS; column, Phenomenex Kinetex F5 2.6 μm 100 Å 100 × 4.6 mm; solvent system, Buffer A: 0.1% Formic acid in water and Buffer B: Acetonitrile: Methanol [9:1]. The flow rate was 0.5 mL/min, and the ratio of Buffer A: Buffer B was as follows: 75%/25% at 0 min, 65%/35% at 10 min, 5%/95% at 16.1 min and 20 min, 75%/25% at 16.1 min and 20.1 min and 22 min. Mass Spectrometry: Scan Mode, Full Scan All Ion Fragmentation; Full MS Scan Resolution, 70 000; Full MS Scan Range, 120–1000 m/z; AIF Scan Resolution, 70 000; AIF Scan Range, 80–700 m/z; Normalized Collision Energy, 20, 30, 40 V; Sheath Gas Flow, 35; Aux Gas Flow, 25; Sweep Gas Flow, 5; Spray Voltage (kV), 3.5; Capillary Temp (°C), 300; S-lens RF Level, 100; and Aux Gas Heater temp (°C), 450. The concentration of each compound was calculated by normalization of the peak area to that of the standard curve of its corresponding analytical standard.

Biofilm assay in plant extracts and root exudates

The plants were grown hydroponically in 5-gallon plastic pails in the presence of 22.5 ppm N. Freeze-dried root exudates were prepared as in flavonoid measurements (see above). Following exudate collection, plants were harvested and ground into fine powder in liquid nitrogen. In the biofilm assay, freeze-dried root exudates were dissolved in 5 mL of sterile milli-Q water supplemented with 1% sucrose and 1% mannitol to support bacteria growth. The plant extracts were dissolved in 40 times (2.5%

weight/volume) sterile milli-Q water. The suspension was filter-sterilized with a 0.45 μm Corning 50 mL tube top vacuum filter and used to culture the bacteria in the biofilm assay.

Photosynthesis and chlorophyll measurement

Net CO_2 assimilation rate, stomatal conductance and transpiration rate were measured simultaneously at the first hour in the morning (9–10 a.m.) in 75-day-old plants using a LI-COR 6400—40 gas exchange instrument. The leaf cuvette was set at 1200 μmol/m²/s photosynthetic photon flux density, 25 °C and a relative humidity of 70%. For the chlorophyll measurement, the same leaf used for photosynthesis measurement was collected and freeze-dried for chlorophyll assay: 50 mg of the leaf were ground with liquid nitrogen and dissolved in 1 mL of 80% acetone (v/v) for 15–30 min. The samples were then centrifuged at 2500 g for 15 min, and the supernatant was transferred to a new tube. Another 1 mL of 80% acetone was added to the pellet to extract the remaining chlorophyll. The supernatant from both acetone extractions was polled together for absorbance measurement at 663 and 645 nm (Biotek Synergy Mx plate reader) using 80% acetone as blank control. The calculation of chlorophyll a, chlorophyll b and total chlorophyll was previously described (Anie and Ar No N, 1949).

Total nitrogen content measurement

Rice dry seeds harvested from 22.5 ppm N were analysed at the UC Davis Analytical Laboratory for the total nitrogen content using combustion method: https://anlab.ucdavis.edu/analysis/Plant/522.

16S metagenomic sampling

Kitaake and crispr plants were grown in soil 'Veggie Mix' for 8 weeks. A 10-cm segment of the root, which is about 5 cm below the root—shoot junction, was harvested after shaking off the loosely attached soil. Rhizosphere, rhizoplane and endosphere were separated as described previously (Edwards et al., 2015). For DNA extraction, the rhizosphere and rhizoplane samples were first homogenized with three 2 mm metal beads in a 2 mL Eppendorf tube: 1200 g for 180 s for the rhizosphere samples and 1200 g for 90 s for the rhizoplane samples using a SPEX SamplePrep 2010 Geno/Grinder. The endosphere samples were ground into powder in liquid nitrogen. All the homogenized samples were further extracted by DNeasy PowerSoil Kit (QIAGEN) according to the manufacturer's instructions.

16S metagenomic sequencing

Primers 799F and 1193R were used to amplify the V5-V7 domain of the 16S rRNA by Kapa2G Robust Hot Start Polymerase (Kapa Biosystems). PCR conditions were as follows: an initial incubation at 95 °C for 3 min, followed by 28 cycles of 95 °C for 45 s, 50 °C for 30 s, 72 °C for 30 s and a final extension of 72 °C for 3 min. In step two, each sample was barcoded with a unique forward and reverse barcode primers and the PCR conditions were as follows: an initial incubation at 95 °C for 3 min, followed by 9 cycles of 95 °C for 30 s, 58 °C for 30 s, 72 °C for 30 s and a final extension of 72 °C for 3 min. The library was quantified via qPCR followed by 300-bp paired-end sequencing using an Illumina MiSeq instrument (Illumina) in the Genome Center DNA Technologies Core, University of California, Davis. Target

amplification, barcoding, and library preparation steps were performed by the UC Davis Host Microbe Systems Biology Core Facility.

16S metagenomic analysis

Briefly, sequences were demultiplexed and primers were trimmed using dbcAmplicon (https://github.com/msettles/dbcAmplicons). The remaining sequence processing occurred in the dada2 version 1.12.1 R package (Callahan et al., 2016), beginning with forward and reverse reads trimming to 270 bp and 180 bp, respectively, following manual inspection of read quality profiles. Forward and reverse reads were filtered to allow a maximum of two expected errors. After error estimation and sample inference, forward and reverse reads were merged, and a sequence table was generated for unique sequence (actual sequence variants or ASVs) and sequence counts per sample. Chimeras were removed, and we assigned taxonomy to genus level using the Silva reference database version 138.1 (Quast et al., 2013). Assignments to species were based on exact sequence matching between AVS and sequences references strains. We removed ASVs that could not be classified as bacteria, as well as sequence variant singletons or shorter than 350 bp. We filtered samples with fewer than 9500 sequences (1 sample), as well as 7 bulk soil samples and 19 rhizosphere samples that had suspiciously similar taxonomic composition independent of compartment and genotype (Figure S4b). Upon deeper investigation, the 26 samples flagged for removal comprised 5089 taxa seen in more than 1 sample. Over 99.7% of these ASVs (5078) were not found in the remaining 73 samples. The final QC'ed dataset represented 73 samples and 4562 ASVs. Bacterial functional classification was estimated using FAPROTAX v 1.2.4 with default parameter values (Louca et al., 2016). The observed ASV richness was estimated from rarefied libraries (depth of 9988 sequences per library), due to the positive correlation between sequencing depth and richness. Beta-diversity was estimated from unrarefied libraries following Hellinger's transformation to down-weight abundant ASVs (Legendre and Gallagher, 2001), with the Bray–Curtis distance metric in the vegan R package (Oksanen, 2019). The raw sequencing data are available https://figshare.com/articles/dataset/raw_FASTQ/17147837.

Statistical analysis

Univariate and multivariate statistics tested whether plant genotype significantly modified the plant-associated bacterial community. Statistical differences in ASV richness between genotypes were determined using the Wilcoxon rank test from rarefied libraries. Factor significance of plant compartment and genotype was determined using a permutational analysis of variance and visualized using principal coordinates analysis. Centroids for each treatment were estimated based on coordinate means. To determine whether individual genera were differentially abundant between genotypes, we calculated generalized linear models with a negative binomial distribution using shrinkage estimation for dispersions in the commonly used DESeq2 package in R (Love et al., 2014). The Wald test P-values were adjusted for multiple comparisons using Benjamini–Hochberg. The impact of genotype on putative nitrogen fixer relative abundance was evaluated with the Wilcoxon rank test across the three compartments. We also modelled predicted N-fixer richness in a two-way ANOVA with plant compartment and genotype as factors. All analyses were conducted in R with, and significance was determined at alpha < 0.05. When linear models were constructed, the data met the assumptions of normality through the investigation of qqplots and Shapiro–Wilk tests.

Isolation of potential nitrogen-fixing bacteria

Root segments (5–10 cm below ground) were harvested from 16-week-old *crispr* plants grown in 22.5 ppm N. Three individual roots were combined and ground up in a mortar and pestle after removing attached soil particle by vortexing. The tissues were filtered through a cheesecloth and dissolved in 50 mL sterile water. A 10^{-4} dilution of the original solution was plated on Jensen's N-free medium containing 1.5% agar and cultured for 7 day at 28 °C. Individual colonies were picked up and grown on fresh Jensen's N-free medium for the second selection. Eighty random colonies that survived the second selection were tested for their biofilm formation in the presence of apigenin. For the identification of the bacteria, primers pair 27YMF: AGRGTTYGA-TYMTGGCTCAG and 515R: TTACCGCGGCKGCTGGCAC or 799F: AACMGGATTAGATACCCKG and 1492R: RGYTACCTTGT-TACGACTT was used to amplify the 16S region for sequencing and search against the EzBioCloud (Yoon et al., 2017).

Phylogenetic analysis of *CYP75B3* and *CYP75B4* orthologs in major crops

Orthologous genes of CYP75B3 and CYP75B4 were selected using the online tool PLAZA (Van Bel et al., 2018): https://bioinformatics.psb.ugent.be/plaza/. The phylogenetic tree was constructed through Interactive Tree Of Life (iTOL) (Letunic and Bork, 2019).

Conflict of interest

The authors declare that the research was conducted in the absence of any commercial or financial relationships that could be construed as a potential conflict of interest. The University of California, Davis has applied for patents related to the work in this article.

Author contributions

E.B. and D.Y. conceived the project with the help of H.Y.S. Experiments were designed by E.B. and D.Y. and performed by D.Y. CRISPR constructs were designed and prepared by H.T. Metagenomics analysis was performed by L.C.C. Flavonoid measurements were performed by T.Y.F. and J.I.O. The manuscript was written by E.B. and D.Y. with input from all authors.

References

Anie, D. and Ar No N, L.I. (1949) Copper enzymes in isolated chloroplasts. Polyphenoloxidase in Beta Vulgaris. *Plant Physiol.* **24**, 1–15.

Backman, T.W.H., Cao, Y. and Girke, T. (2011) ChemMine tools: An online service for analyzing and clustering small molecules. *Nucleic Acids Res.* **39**, W486–W491.

Callahan, B.J., McMurdie, P.J., Rosen, M.J., Han, A.W., Johnson, A.J.A. and Holmes, S.P. (2016) DADA2: High-resolution sample inference from Illumina amplicon data. *Nat. Methods*, **13**, 581–583.

Čermák, T., Curtin, S.J., Gil-Humanes, J., Čegan, R., Kono, T.J.Y., Konečná, E., Belanto, J.J. *et al.* (2017) A multipurpose toolkit to enable advanced genome engineering in plants. *Plant Cell*, **29**, 1196–1217.

Cesco, S., Mimmo, T., Tonon, G., Tomasi, N., Pinton, R., Terzano, R., Neumann, G. *et al.* (2012) Plant-borne flavonoids released into the rhizosphere: impact on soil bio-activities related to plant nutrition. A review. *Biol. Fertil. Soils*, **48**, 123–149.

Cocking, E.C., Stone, P.J. and Davey, M.R. (2006) Intracellular colonization of roots of Arabidopsis and crop plants by Gluconacetobacter diazotrophicus. *Vitr. Cell. Dev. Biol. - Plant*, **42**, 74–82.

Edwards, J., Johnson, C., Santos-Medellín, C., Lurie, E., Podishetty, N.K., Bhatnagar, S., Eisen, J.A. *et al.* (2015) Structure, variation, and assembly of the root-associated microbiomes of rice. *Proc. Natl. Acad. Sci. USA*, **112**, E911–E920.

Essien, E.E., Said Abasse, K., Côté, A., Mohamed, K.S., Baig, M.M.F.A., Habib, M. *et al.* (2020) Drinking-water nitrate and cancer risk: A systematic review and meta-analysis. *Arch. Environ. Occup. Health*, **77**, 1–17.

Flemming, H.-C. and Wingender, J. (2010) The biofilm matrix. *Nat. Rev. Microbiol.* **8**, 623–633.

Flemming, H.C., Wingender, J., Szewzyk, U., Steinberg, P., Rice, S.A. and Kjelleberg, S. (2016) Biofilms: An emergent form of bacterial life. *Nat. Rev. Microbiol.* **14**, 563–575.

Fowler, D., Coyle, M., Skiba, U., Sutton, M.A., Cape, J.N., Reis, S., Sheppard, L.J. *et al.* (2013) The global nitrogen cycle in the twenty-first century. *Philos. Trans. R. Soc. B Biol. Sci.* **368**, 20130164.

Genevaux, P., Muller, S. and Bauda, P. (1996) A rapid screening procedure to identify mini-Tn10 insertion mutants of *Escherichia coli* K-12 with altered adhesion properties. *FEMS Microbiol. Lett.* **142**, 27–30.

Glendining, M.J., Dailey, A.G., Williams, A.G., Evert, F.K.v., Goulding, K.W.T. and Whitmore, A.P. (2009) Is it possible to increase the sustainability of arable and ruminant agriculture by reducing inputs? *Agr. Syst.* **99**, 117–125.

Haichar, F.e.Z., Heulin, T., Guyonnet, J.P. and Achouak, W. (2016) Stable isotope probing of carbon flow in the plant holobiont. *Curr. Opin. Biotechnol.* **41**, 9–13.

Hartwig, U.A. and Phillips, D.A. (1991) Release and modification of nod-gene-inducing flavonoids from alfalfa seeds. *Plant Physiol.* **95**, 804–807.

Hartwig, U.A., Joseph, C.M. and Phillips, D.A. (1991) Flavonoids released naturally from alfalfa seeds enhance growth rate of Rhizobium meliloti. *Plant Physiol.* **95**, 797–803.

Hyung Ko, J., Gyu Kim, B. and Joong-Hoon, A. (2006) Glycosylation of flavonoids with a glycosyltransferase from Bacillus cereus. *FEMS Microbiol. Lett.* **258**, 263–268.

Jensen, H.L. (1942) Nitrogen fixation in leguminous plants. II. Is symbiotic nitrogen fixation influenced by Azotobacter? *Proc. Linn. Soc. New South Wales*, **67**, 205–212.

Kent, P.N., W., F.J. and R., L.S. (1986) A plant flavone, luteolin, induces expression of rhizobium meliloti nodulation genes. *Science*, **233**, 977–980.

Khush, G.S. (2001) Green revolution: The way forward. *Nat. Rev. Genet.* **2**, 815–822.

Lam, P.Y., Liu, H. and Lo, C. (2015) Completion of tricin biosynthesis pathway in rice: Cytochrome P450 75B4 is a unique chrysoeriol 5′-hydroxylase. *Plant Physiol.* **168**, 1527–1536.

Lam, P.Y., Tobimatsu, Y., Takeda, Y., Suzuki, S., Yamamura, M., Umezawa, T. and Lo, C. (2017) Disrupting flavone synthase II alters lignin and improves biomass digestibility. *Plant Physiol.* **174**, 972–985.

Lam, P.Y., Lui, A.C.W., Yamamura, M., Wang, L., Takeda, Y., Suzuki, S., Liu, H. *et al.* (2019) Recruitment of specific flavonoid B-ring hydroxylases for two independent biosynthesis pathways of flavone-derived metabolites in grasses. *New Phytol.* **223**, 204–219.

Legendre, P. and Gallagher, E.D. (2001) Ecologically meaningful transformations for ordination of species data. *Oecologia*, **129**, 271–280.

Letunic, I. and Bork, P. (2019) Interactive Tree of Life (iTOL) v4: recent updates and new developments. *Nucleic Acids Res.* **47**, W256–W259.

Li, S., Tian, Y., Wu, K., Ye, Y., Yu, J., Zhang, J., Liu, Q. *et al.* (2018) Modulating plant growth–metabolism coordination for sustainable agriculture. *Nature*, **560**, 595–600.

Liu, F., Wang, P., Zhang, X., Li, X., Yan, X., Fu, D. and Wu, G. (2018) The genetic and molecular basis of crop height based on a rice model. *Planta*, **247**, 1–26.

Love, M.I., Huber, W. and Anders, S. (2014) Moderated estimation of fold change and dispersion for RNA-seq data with DESeq2. *Genome Biol.* **15**, 1–21.

Louca, S., Parfrey, L.W. and Doebeli, M. (2016) Decoupling function and taxonomy in the global ocean microbiome. *Science*, **353**, 1272–1277.

Meech, R., Hu, D.G., McKinnon, R.A., Mubarokah, S.N., Haines, A.Z., Nair, P.C., Rowland, A. *et al.* (2019) The UDP-Glycosyltransferase (UGT) superfamily: New members, new functions, and novel paradigms. *Physiol. Rev.* **99**, 1153–1222.

Meneses, C.H.S.G., Rouws, L.F.M., Simões-Araújo, J.L., Vidal, M.S. and Baldani, J.I. (2011) Exopolysaccharide production is required for biofilm formation and plant colonization by the nitrogen-fixing endophyte Gluconacetobacter diazotrophicus. *Mol. Plant Microbe Interact.* **24**, 1448–1458.

Oelze, J. and Klein, G. (1996) Control of nitrogen fixation by oxygen in purple nonsulfur bacteria. *Arch. Microbiol.* **165**, 219–225.

Oksanen, J. (2019) *vegan: Community Ecology Package*.

Pabuayon, I.M., Yamamoto, N., Trinidad, J.L., Longkumer, T., Raorane, M.L. and Kohli, A. (2016) Reference genes for accurate gene expression analyses across different tissues, developmental stages and genotypes in rice for drought tolerance. *Rice*, **9**, 32.

Peng, M., Shahzad, R., Gul, A., Subthain, H., Shen, S., Lei, L., Zheng, Z. *et al.* (2017) Differentially evolved glucosyltransferases determine natural variation of rice flavone accumulation and UV-tolerance. *Nat. Commun.* **8**, 1–12.

Quast, C., Pruesse, E., Yilmaz, P., Gerken, J., Schweer, T., Yarza, P., Peplies, J. *et al.* (2013) The SILVA ribosomal RNA gene database project: improved data processing and web-based tools. *Nucleic Acids Res.* **41**, D590.

Ramos, H.J.O., Roncato-Maccari, L.D.B., Souza, E.M., Soares-Ramos, J.R.L., Hungria, M. and Pedrosa, F.O. (2002) Monitoring Azospirillum-wheat interactions using the gfp and gusA genes constitutively expressed from a new broad-host range vector. *J. Biotechnol.* **97**, 243–252.

Rausher, M.D. (2006) The evolution of flavonoids and their genes. In *The Science of Flavonoids* (Grotewold, E., ed), pp. 175–211. New York, NY: Springer New York.

Rosenblueth, M., Ormeño-Orrillo, E., López-López, A., Rogel, M.A., Reyes-Hernández, B.J., Martínez-Romero, J.C., Reddy, P.M. *et al.* (2018) Nitrogen fixation in cereals. *Front. Microbiol.* **9**, 1794.

Slobodníková, L., Fialová, S., Rendeková, K., Kováč, J. and Mučaji, P. (2016) Antibiofilm activity of plant polyphenols. *Molecules*, **21**, 1717.

Thompson, R.L., Lassaletta, L., Patra, P.K., Wilson, C., Wells, K.C., Gressent, A., Koffi, E.N. *et al.* (2019) Acceleration of global N2O emissions seen from two decades of atmospheric inversion. *Nat. Clim. Chang.* **9**, 993–998.

Udvardi, M. and Poole, P.S. (2013) Transport and metabolism in legume-rhizobia symbioses. *Annu. Rev. Plant Biol.* **64**, 781–805.

Van Bel, M., Diels, T., Vancaester, E., Kreft, L., Botzki, A., Van De Peer, Y., Coppens, F. *et al.* (2018) PLAZA 4.0: an integrative resource for functional, evolutionary and comparative plant genomics. *Nucleic Acids Res.* **46**, D1190–D1196.

Vestby, L.K., Grønseth, T., Simm, R. and Nesse, L.L. (2020) Bacterial biofilm and its role in the pathogenesis of disease. *Antibiotics*, **9**, 59.

Vogt, T. (2010) Phenylpropanoid biosynthesis. *Mol. Plant*, **3**, 2–20.

Wang, D., Xu, A., Elmerich, C. and Ma, L.Z. (2017) Biofilm formation enables free-living nitrogen-fixing rhizobacteria to fix nitrogen under aerobic conditions. *ISME J.* **11**, 1602–1613.

Watson, B.S., Bedair, M.F., Urbanczyk-Wochniak, E., Huhman, D.V., Yang, D.S., Allen, S.N., Li, W. *et al.* (2015) Integrated metabolomics and transcriptomics reveal enhanced specialized metabolism in medicago truncatula root border cells. *Plant Physiol.* **167**, 1699–1716.

Wen, W., Alseekh, S. and Fernie, A.R. (2020) Conservation and diversification of flavonoid metabolism in the plant kingdom. *Curr. Opin. Plant Biol.* **55**, 100–108.

Wisniewski-Dyé, F., Borziak, K., Khalsa-Moyers, G., Alexandre, G., Sukharnikov, L.O., Wuichet, K., Hurst, G.B. *et al.* (2011) Azospirillum genomes reveal transition of bacteria from aquatic to terrestrial environments. *PLoS Genet.* **7**, e1002430.

Withers, P.J.A., Neal, C., Jarvie, H.P. and Doody, D.G. (2014) Agriculture and eutrophication: where do we go from here? *Sustainability*, **6**, 5853–5875.

Yoneyama, T., Tanno, F., Tatsumi, J. and Mae, T. (2016) Whole-plant dynamic system of nitrogen use for vegetative growth and grain filling in rice plants (*Oryza sativa* L.) as revealed through the production of 350 grains from a germinated seed over 150 days: a review and synthesis. *Front Plant Sci.* **7**, 1151.

Yoon, S.H., Ha, S.M., Kwon, S., Lim, J., Kim, Y., Seo, H. and Chun, J. (2017) Introducing EzBioCloud: a taxonomically united database of 16S rRNA gene sequences and whole-genome assemblies. *Int. J. Syst. Evol. Microbiol.* **67**, 1613–1617.

Yoshida, S., Forno, D.A., Cock, J.H. and Gomez, K.A. (1976) Routine procedure for growing rice plants in culture solution. In *Laboratory Manual for Physiological Studies of Rice*(Yoshida, S., Forno, D.A. and Cock, J.H., eds), pp. 61–66. Los Baños: International Rice Research Institute.

Yu, P., He, X., Baer, M., Beirinckx, S., Tian, T., Moya, Y.A.T., Zhang, X. *et al.* (2021) Plant flavones enrich rhizosphere Oxalobacteraceae to improve maize performance under nitrogen deprivation. *Nat. Plants*, **7**, 481–499.

Zhang, J., Subramanian, S., Stacey, G. and Yu, O. (2009) Flavones and flavonols play distinct critical roles during nodulation of Medicago truncatula by *Sinorhizobium meliloti*. *Plant J.* **57**, 171–183.

Zhu, Q., Yu, S., Zeng, D., Liu, H., Wang, H., Yang, Z., Xie, X. *et al.* (2017) Development of "Purple Endosperm Rice" by engineering anthocyanin biosynthesis in the endosperm with a high-efficiency transgene stacking system. *Mol. Plant*, **10**, 918–929.

Supporting information

Additional supporting information may be found online in the Supporting Information section at the end of the article.

Figure S1 Workflow of the chemical screening and hits validation.

Figure S2 Agronomic traits of the 75-days-old *crispr* lines grown under 22.5 ppm N regime.

Figure S3 Comparison of the yield and seed nitrogen content in different nitrogen conditions.

Figure S4 Potential nitrogen-fixing bacteria isolated from the *crispr* lines respond to apigenin.

Figure S5 Comparison of root microbiota in Kitaake and the *crispr* line.

Figure S6 Nitrogen-fixing bacteria predicted by FAPROTAX.

Figure S7 Unrooted phylogenetic tree of CYP75B3 and CYP75B4 homologues in major crops.

Table S1 Soil cation and organic material contents (*)Soil Exchangeable Cation; (CEC) Cation Exchange Capacity; (OM) Organic Material.

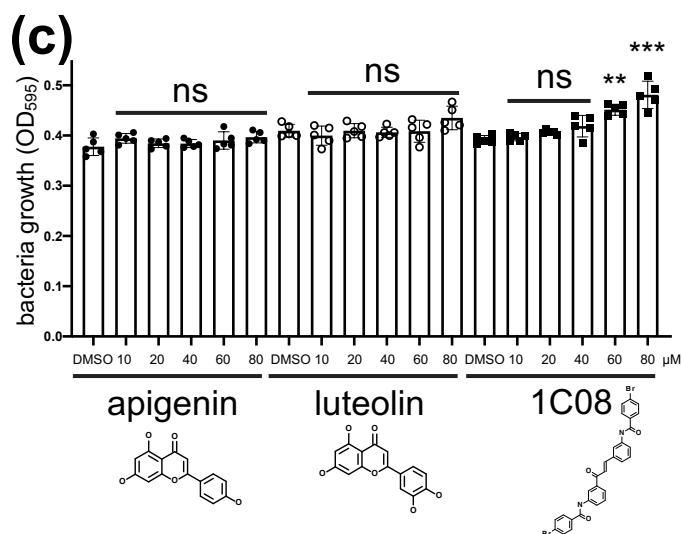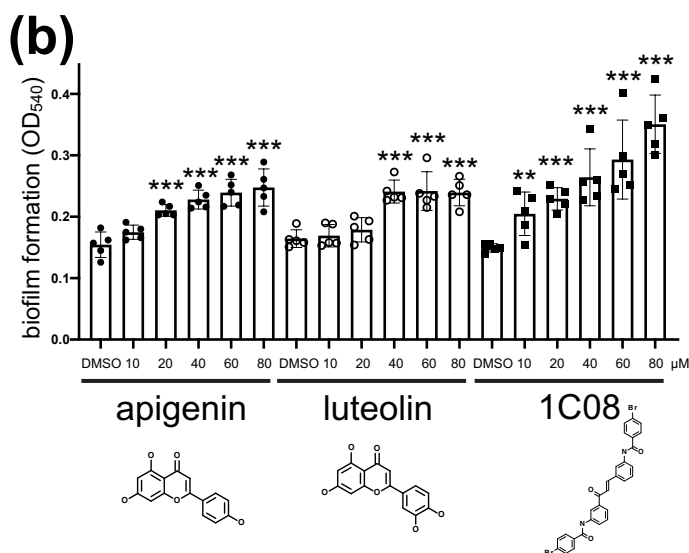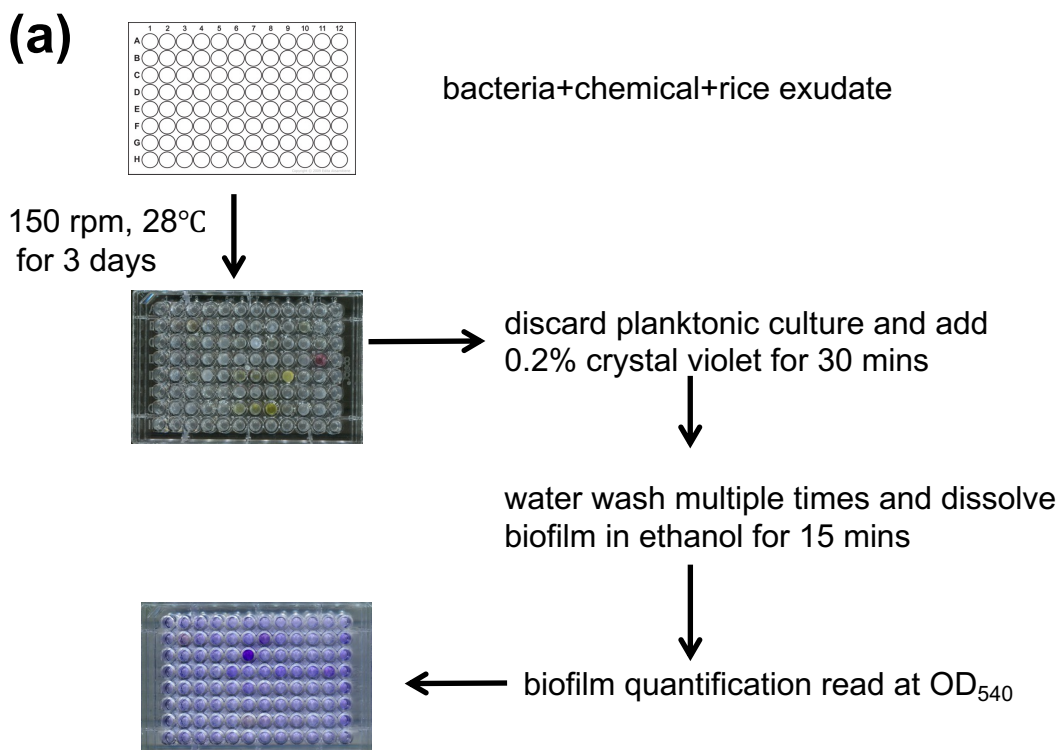**Table S2** Rice medium.

Table S3 List of primers.

Figure S1 Workflow of the chemical screening and hits validation. (a) Workflow of the chemical screening for biofilm regulators in nitrogen-fixing bacteria. The dose dependent induction of biofilm by apigenin, luteolin **(b)** without impacting the growth of the nitrogen-fixing bacteria *Gluconacetobacter diazotrophicus* **(c)**. Data is shown by a mean±s.d. (n=5). ns: not significant, **P<0.01 and ***P<0.001 (One-way ANOVA followed by Dunnett's test compared with DMSO control).
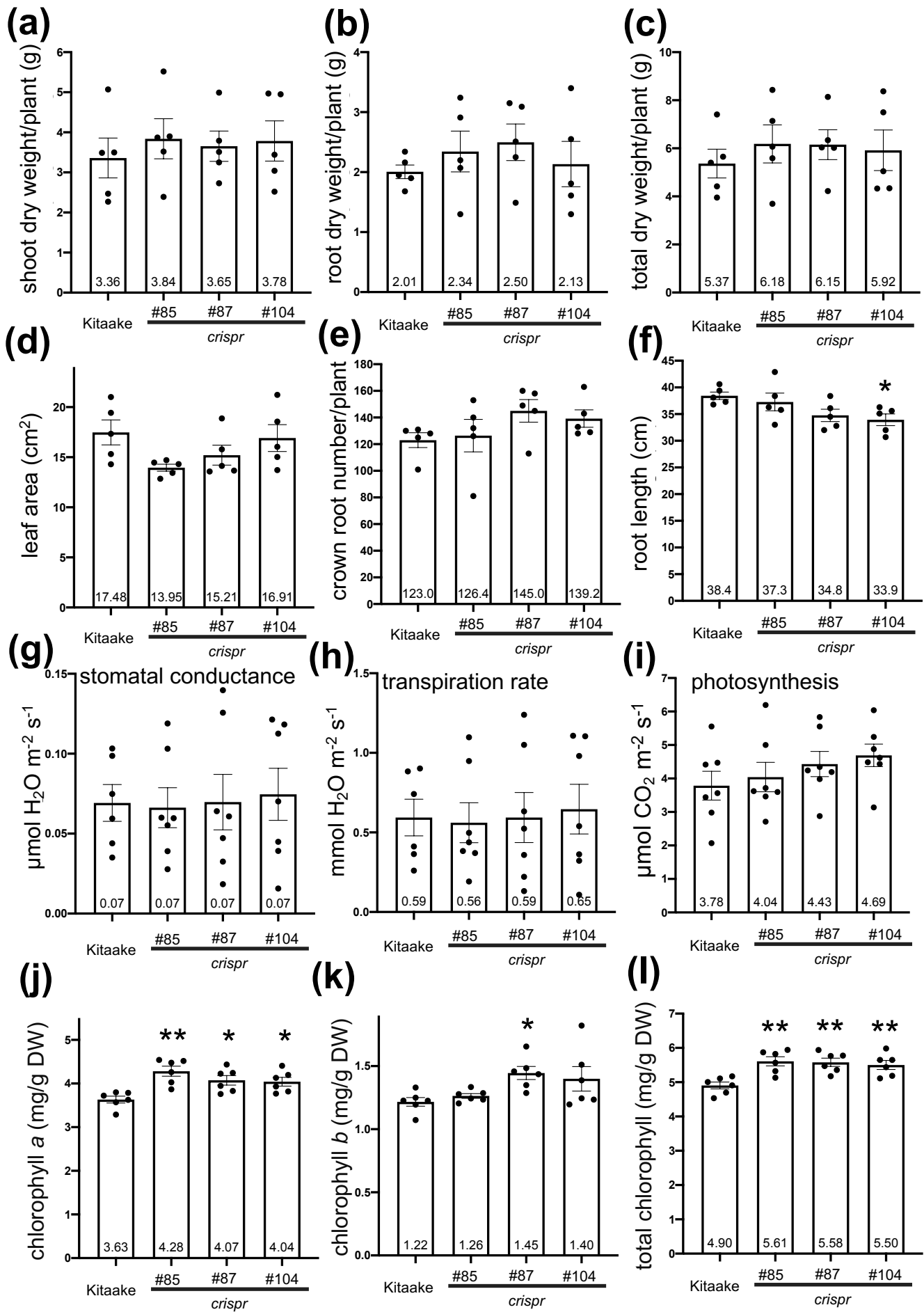
Figure S2 Agronomic traits of the 75-days-old *crispr* lines grown under 22.5ppm N regime. (**j**), (**k**), (**l**) The *crispr* lines had a significant higher level of chlorophyll content. Data is presented as mean±s.e. (n=5 to 7). * P<0.05,**P<0.01 (One-way ANOVA followed by Dunnett's test compared with Kitaake control).
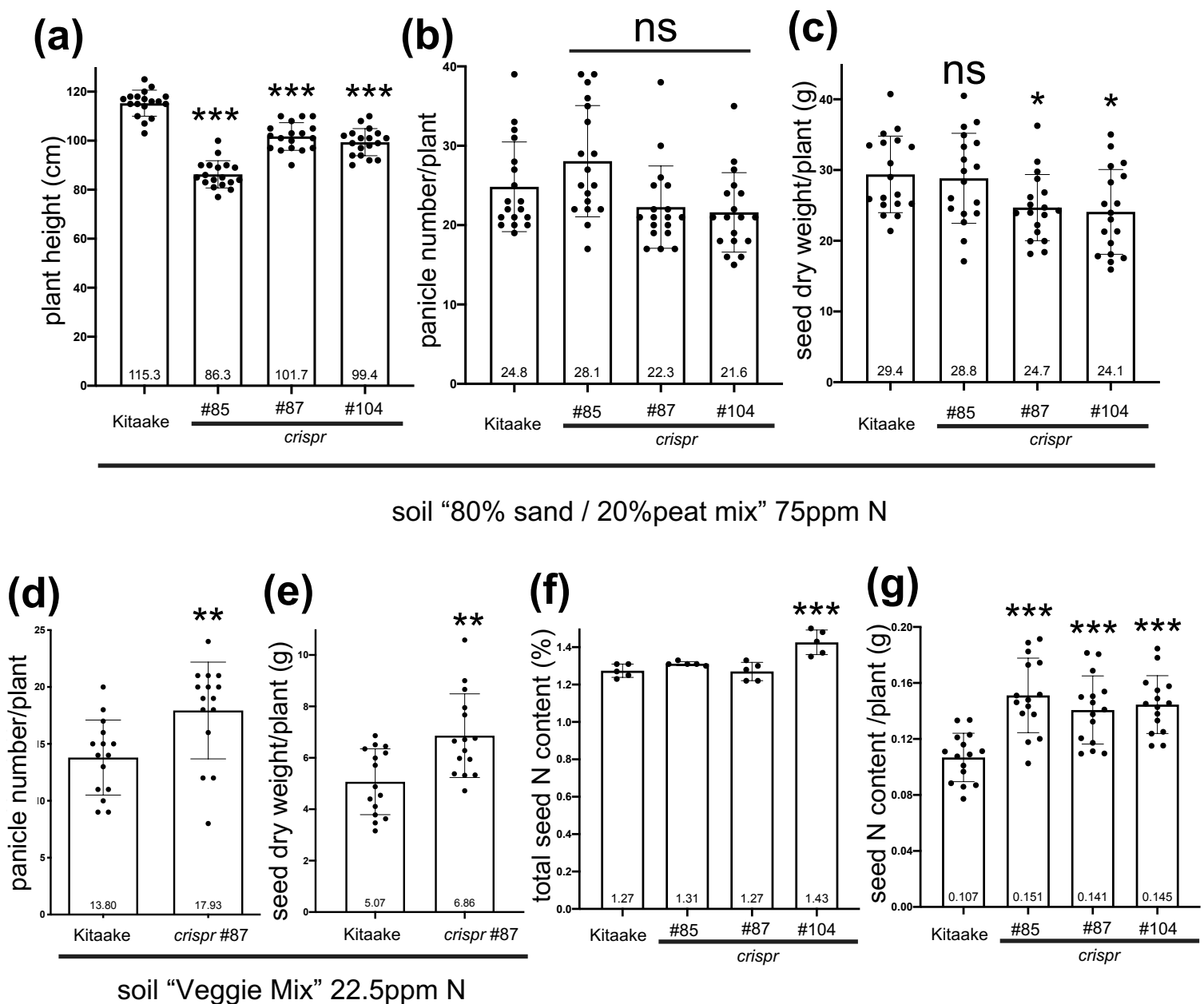
Figure S3 Comparison of the yield and seed nitrogen content in different nitrogen conditions. The *crispr* lines are shorter but does not produced more seeds under the optimal nitrogen condition (75ppm). When grown at the optimal nitrogen condition (75ppm N), the *crispr* lines have shorter plant height **(a)** with normal panicle numbers **(b)**, and produce similar or lower dry weight of seeds **(c)**. Data is shown by a mean±s.d. (n=18). ns: not significant, *P<0.05, and ***P<0.001 (One-way ANOVA followed by Dunnett's test compared with Kitaake control). The *crispr* #87 produce more panicle numbers **(d)** and seeds **(e)** than Kitaake in the soil "Veggie Mix" under 22.5ppm N regime. The same soil was used for 16S sequencing. Data is shown by a mean±s.d. (n=15). **P<0.01 (Two-sided Student *t*-test compared with Kitaake control). **(f)** The total nitrogen content in rice seed growing under limiting nitrogen condition. Data is presented as mean±s.d. (n=5). ***P<0.001 (One-way ANOVA followed by Dunnett's test compared with Kitaake control). The total nitrogen content was analyzed at UC Davis Analytical Lab using Total Nitrogen and Carbon-Combustion Method. **(g)** The *crispr* lines have significant higher level of seed nitrogen per plant when growing under limiting nitrogen condition. Data is presented as mean±s.d. (n=15). ***P<0.001 (One-way ANOVA followed by Dunnett's test compared with Kitaake control).
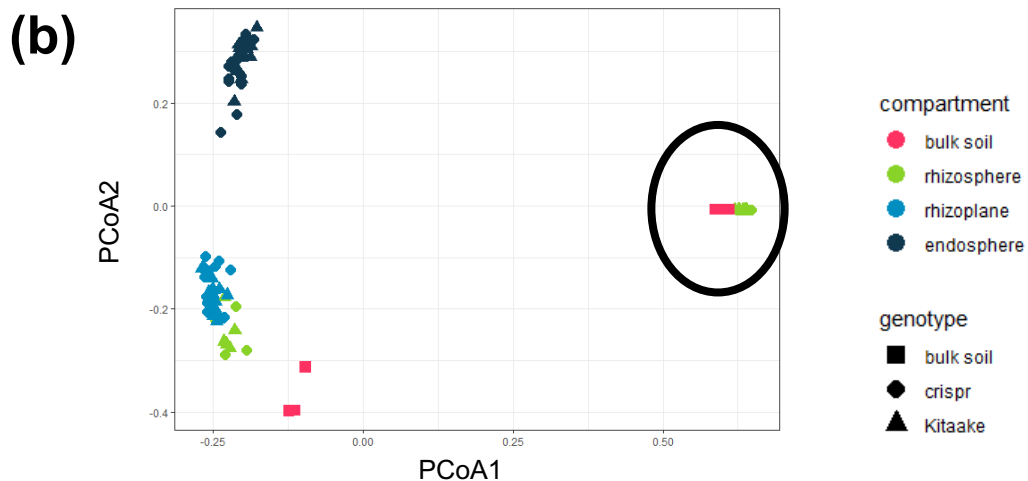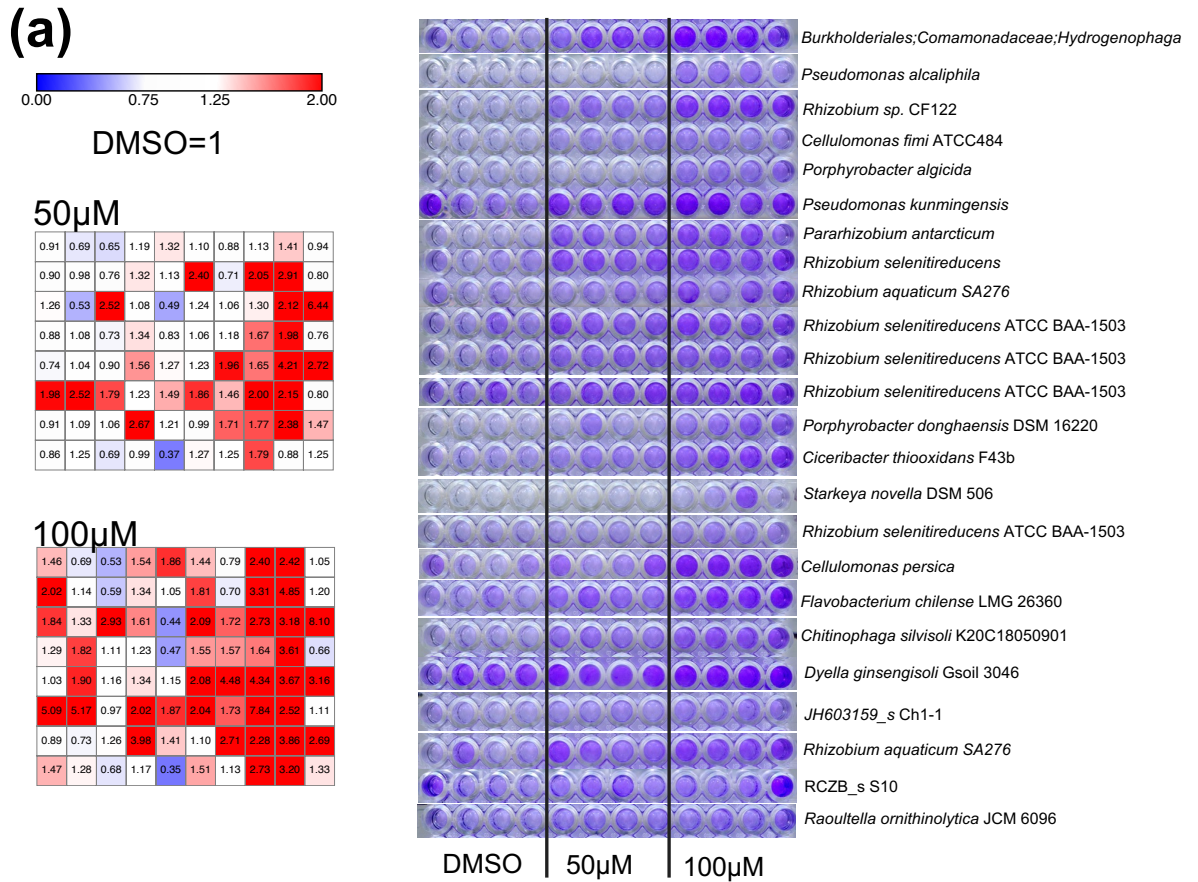
Figure S4 Potential nitrogen-fixing bacteria isolated from the *crispr* lines respond to apigenin. The culturable nitrogen-fixing bacteria from the rhizoplane and endophyte of the *crispr* lines were isolated from 16-week-old *crispr* line grown in 22.5 ppm N medium **(a)**. Biofilm were quantified by crystal violet staining and normalized to the value of the DMSO control for each bacterium. The heatmap was generated by the mean value of 4 biological replicates. The identification of each bacterium was performed by sequencing the PCR using the 16S degenerate primers, and searching in the database: https://www.ezbiocloud.net/identify. **(b)** Principal coordinates analysis (PCoA) used to remove 26 bulk soil and rhizosphere samples from the dataset, which are circled. These data points deviate from the gradual transition of bacterial composition from soil to rhizosphere, rhizoplane and endosphere, which is expected as plant selectively filter associated microbes. Therefore, all downstream analysis excludes these data points.
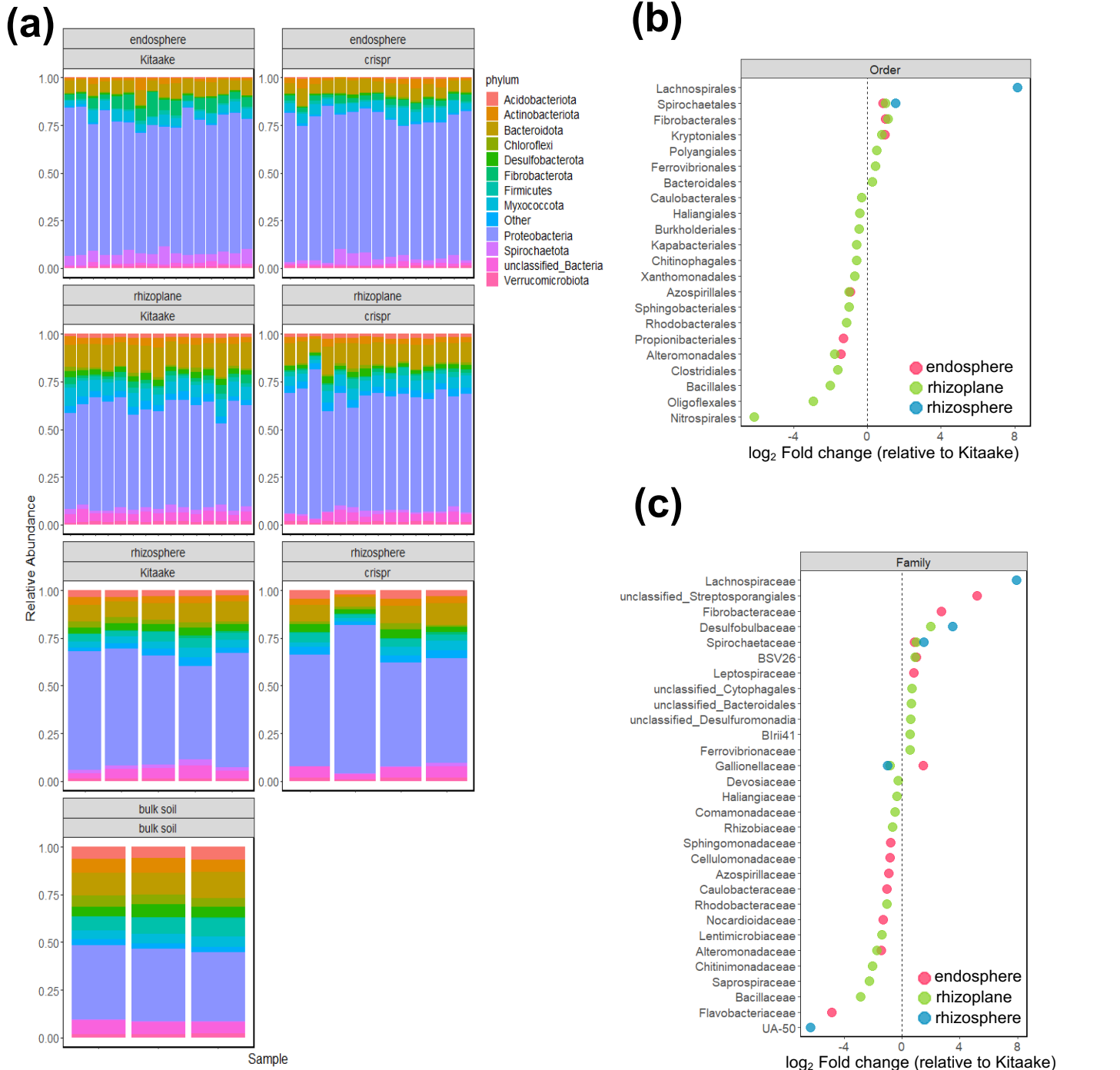
Figure S5 Compasion of root microbiota in Kitaake and the *crispr* line. **(a)** Abundance of bacterial phyla representing more than 1% of libraries across the experiment. All phyla less than <1% have been combined into "other". Order **(b)** and Family **(c)** with a significantly different abundance in the *crispr* line relative to Kitaake control across the three plant compraments. Log2-fold change was calculated from raw sequence counts using generalized linear models with a negative binomial distribution and shrinkage estimation for dispersions. Wald test P-values were adjusted for multiple comparisons using Benjamini-Hochberg and significance was determined at alpha < 0.05. Values greater than 0 indicate order or family that have a significantly higher abundance in the *crispr* genotype relative to Kitaake; whereas, values less than 0 indicate those with a significantly lower abundance in the *crispr* genotype.
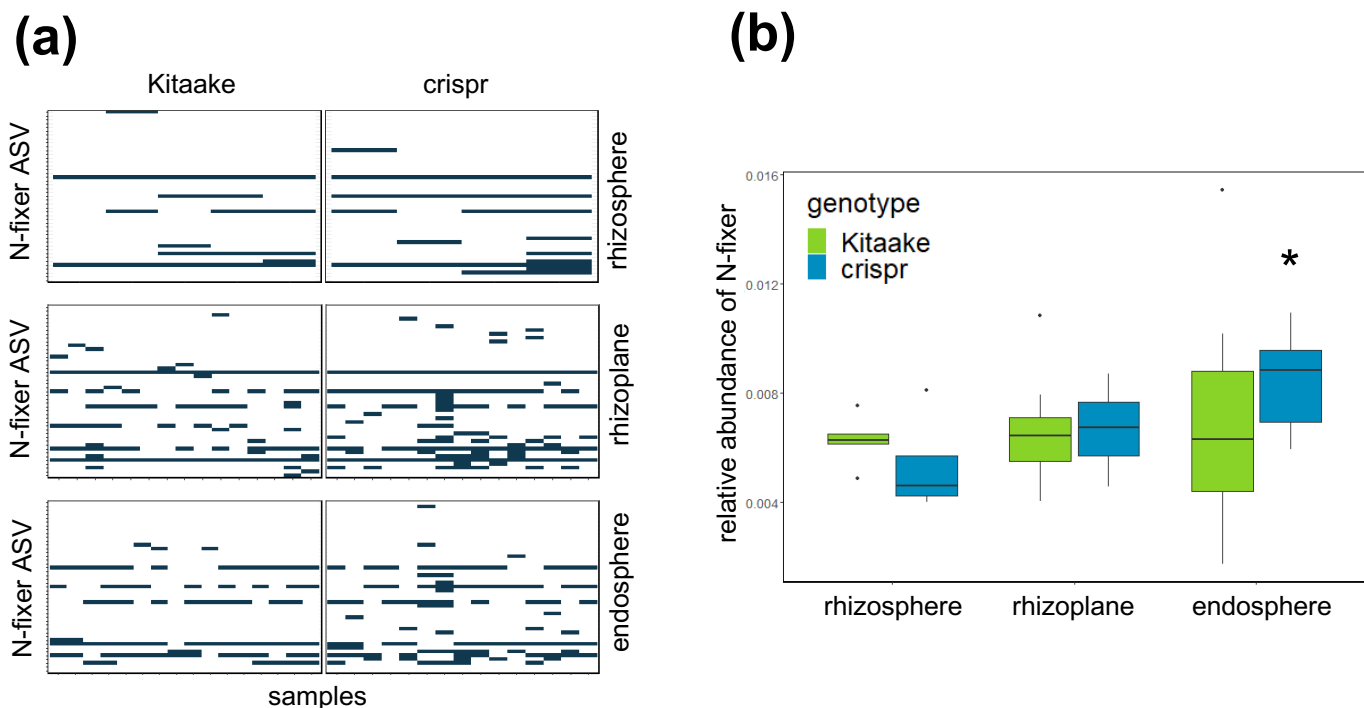
Figure S6 Nitrogen-fixing bacteria predicted by FAPROTAX. **(a)** Pattern of the presence of the nitrogen-fixing bacteria in the rhizosphere, rhizoplane, and endosphere between Kitaake and the *crispr* line. Each column represents a individual sample and each row represents an OTU assigned as nitrogen-fixing bacteria by FAPROTAX. Related to Fig.5 **(e)**. **(b)** Relative abundance of nitrogen-fixing bacterial ASV predicted by FAPROTAX in the rhizosphere, rhizoplane, and endosphere between Kitaake and the *crispr* line. The endosphere of the *crispr* line enriched a significant higher abundance of nitrogen-fixing bacteria than that in the Kitaake control (wilcoxon rank test, W = 175, P = 0.030).
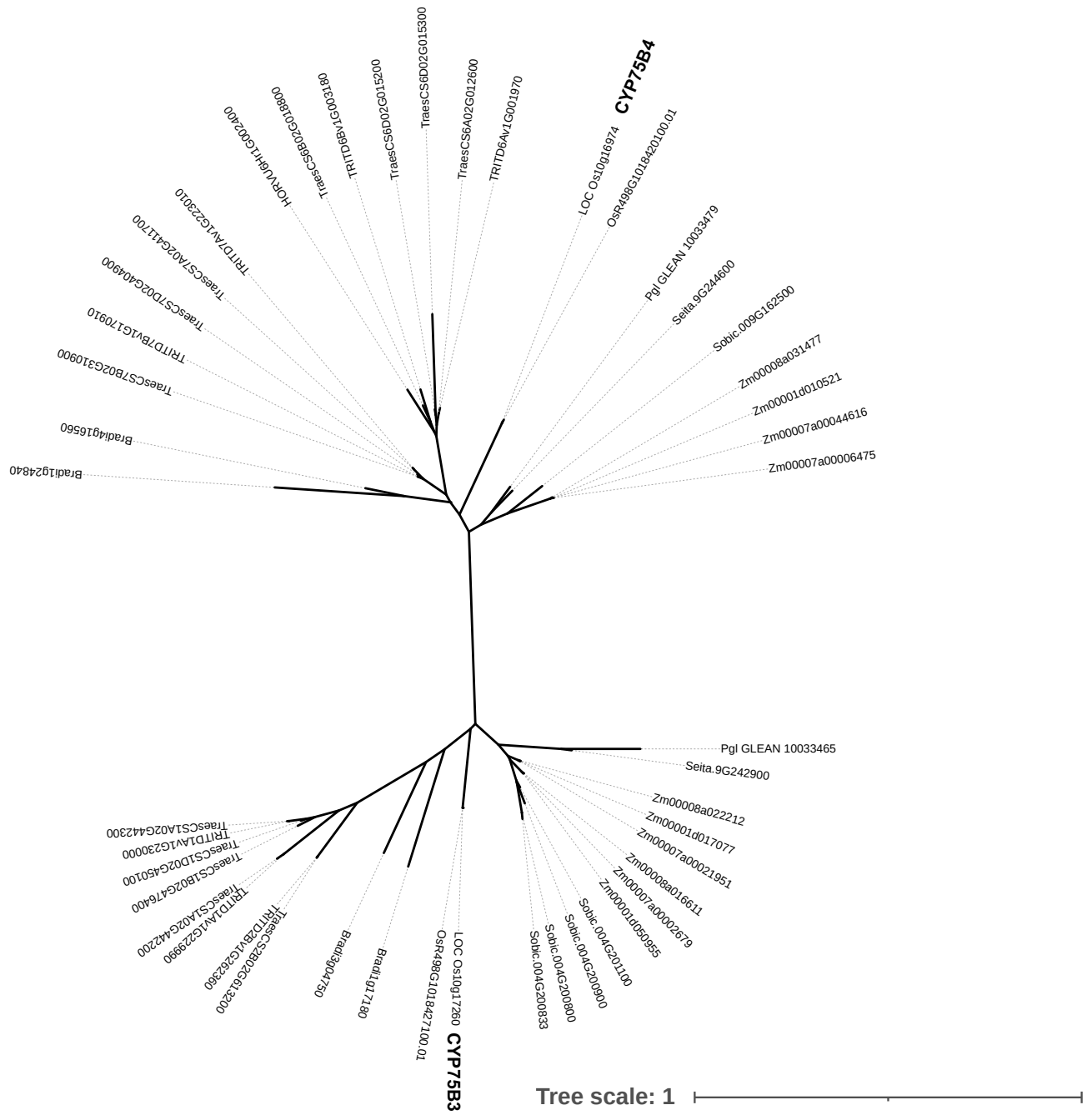
Figure S7 Unrooted phylogenetic tree of CYP75B3 and CYP75B4 homologs in major crops. Homologs of CYP75B3 and CYP75B4 were selected using online tool PLAZA: https://bioinformatics.psb.ugent.be/plaza/. Phylogenetic tree was constructed by Interactive Tree Of Life (iTOL) at https://itol.embl.de/.

Table S1
Soil cation and organic material contents

	Veggie Mix	80%sand/20%peat mix
N (total) (%)	0.084	0.032
NH4-N (ppm)	9.54	7.19
NO3-N (ppm)	0.73	0.41
P (ppm)	26.6	1.7
K (ppm)	192	39
K (meq/100g)*	0.49	0.10
Na (ppm)	77	47
Na (meq/100g)*	0.33	0.20
Ca (meq/100g)*	13.30	4.35
Mg (meq/100g)*	3.39	2.50
CEC (meq/100 mg)	17.52	7.15
OM (%)	6.32	1.28
pH	7.28	6.32

(*)Soil Exchangeable Cation; (CEC) Cation Exchange Capacity;
(OM) Organic Material.

Table S2
Rice medium

Rice medium	Tank A (5 gallon)		Tank B (5 gallon)	
22.5 ppm, 30%N				
	$Ca(NO_3)_2$	293.65g	Monopotassium Phosphate fertilizer (MKP)	300g
	$CaCl_2$	111g	K_2SO_4	445g
	Fe-EDDHA	94.5g	$MgSO_4$	625g
	Zinc EDTA	1.35g	$(NH_4)_2SO_4$	188.8g
	Cu EDTA	0.55g		
	Mn EDTA	13.5g		
	$NaMoO_4$	0.095g		
75 ppm, 100%N				
	$Ca(NO_3)_2$	490g	Monopotassium Phosphate fertilizer (MKP)	300g
	KNO_3	525g	$MgSO_4$	625g
	Fe-EDDHA	94.5g	$(NH_4)_2SO_4$	655g
	Zinc EDTA	1.35g		
	Cu EDTA	0.55g		
	Mn EDTA	13.5g		
	$NaMoO_4$	0.095g		

Table S3
List of primers

Purpose	primer name	sequence (5' to 3')
Vector construction		
gumDpro::GFP	gumDproF	CCTTAATTAAGAAATAACGGGCCACGACGGC
	gumDproR	GGGGTACCGCGCTCACTGTCGACCGTTTTAC
genpro::mCherry	Pac-GentPro-F	TATTTGATGCCTTTAATTAAttgacataagcctgttcggttc
	Luc-GentPro-R	TTTTGGCGTCTTCCATcgttgctgctccataacatcaaac
	LucStart-F	ATGGAAGACGCCAAAAACATAAAGAAAGGC
	Not-Luc-R	CGAATTCGCGCGGCCGCTTACACGGCGATCTTTCCGCCCTTCTTGGCC
qRT-PCR		
CYP75B3	75b3qrtF	GCTTGCGGATGGTCACACTGATG
	75b3qrtR	CATAAGCCGATGGAAGCAGCCTTG
CYP75B4	75b4qrtF	CGGACCAGACGCCAGACAAG
	75b4qrtR	GATGGGAGAAGCCTTGGTACC
Reference gene	Os08g03290qrtF	AATGGCAAGCTTACGGGAATGTC
	Os08g03290qrtR	TGAGGCAGCCTTCTCGATTCTAAC
Reference gene	Os02g06640qrtF	CGAGCCTCTGTTCGTCAAGTATTTG
	Os02g06640qrtR	ACGGACTCGATGGTCCATTAAACC
Reference gene	Os03g13170qrtF	GTATCATCGAGCCGTCGCTTC
	Os03g13170qrtR	CATAGCATTTGCGGCAGATCATC
Genotyping for sequencing		
CYP75B3	75b3criF	AAACCCGCATTTCCCATCGTAC
	75b3criR3	ACCATCTCCTTGAACTCCCTTG
CYP75B4	75b4criF	TAGGTAAGGGATCTCAGGATGG
	75b4criR	TAAGGGCCTTGATTTCCGTGTC

Purpose	primer name	sequence (5' to 3')

[AarI sites, TaU3 promoter, tRNAs, target sequence, sgRNAs, 35S terminator]

Purpose	sequence (5' to 3')
The sequence of synthesized CYP75 multiplex gRNA cassette	cacctgccaggGGACggagagttttaacattgactagcgtgctgataatttgtgagaaataataattga caagtagatactgacatttgagaagagcttctgaactgttattagtaacaaaaatggaaagctgatgcacgg aaaaaggaaagaaaaagccatactttttttaggtaggaaaagaaaaagccatacgagactgatgt ctctcagatgggccgggatctgtctatctagcaggcagcagccctaccaacctcacgggccagcaa ttacgagtccttctaaaacgtcccgccgagggcgcgtggccgtgctgtgcagcagcacgtctaacatta gtcccacctcgccagtttacagggagcagaaccagcttataagcggaggcgcggcaccaagaagcaa caaagcaccagtggtctagtggtagaatagtaccctgccacggtacagacccgggttcgattcccggctgg tgcaTGCGGCAGGTTGCCCAGCACgttttagagctagaaatagcaagttaaaataaggct agtccgttatcaacttgaaaaagtggcaccgagtcggtgcaacaaagcaccagtggtctagtggtagaata gtaccctgccacggtacagacccgggttcgattcccggctggtgcaCCGCTGTTCCGGCTCC GGTTgttttagagctagaaatagcaagttaaaataaggctagtccgttatcaacttgaaaaagtggcaccg Agtcggtgcaacaaagcaccagtggtctagtggtagaatagtaccctgccacggtacagacccgggttc gattcccggctggtgcaACTTCGTGCCGGCGCTCCGGgttttagagctagaaatagcaagtta aaataaggctagtccgttatcaacttgaaaaagtggcaccgagtcggtgcaacaaagcaccagtggtctagtgg tagaatagtaccctgccacggtacagacccgggttcgattcccggctggtgcactcgagtttctccataataatgt gtgagtagttcccagataagggaattagggttcctatagggtttcgctcatgtgttgagcatataagaaacccttag tatgtatttgtatttgtaaaatacttctatcaataaaatttctaattcctaaaaccaaaatccagtactaaaatccagatc ccccgaattacaccggcgAGTGactagcaggtg